Coastal and Hydraulics Laboratory

US Army Corps of Engineers®
Engineer Research and
Development Center

Surge and Wave Island Modeling Studies (SWIMS) Program
Coastal Inlets Research Program (CIRP)

Laboratory Study of Wind Effect on Runup over Fringing Reefs

Report 1: Data Report

Zeki Demirbilek, Okey G. Nwogu, and Donald L. Ward   July 2007

Laboratory Study of Wind Effect on Runup over Fringing Reefs

Report 1: Data Report

Zeki Demirbilek and Donald L. Ward

Coastal and Hydraulics Laboratory
U.S. Army Engineer Research and Development Center
3909 Halls Ferry Road
Vicksburg, MS 39180-6199

Okey G. Nwogu

University of Michigan
Department of Naval Architecture and Marine Engineering
2600 Draper Road
Ann Arbor, MI 48109-2145

Report 1 of a series

Abstract: The report describes experimental data obtained from a wind-wave flume study conducted August-September 2006 at the University of Michigan in Ann Arbor, MI. The study objectives were two-fold: to quantify wind effects on wave runup on fringing reefs of the Pacific Island of Guam and to obtain detailed wave data along a complex reef system consisting of steep slopes and shallow areas for validating wave breaking, dissipation, wave setup and runup capabilities of a Boussinesq-type wave model. An idealized 1:64 model of a two-dimensional fringing reef, representative of the reef systems along the southeast coast of island of Guam, was built in the flume. The reef cross-sectional profile consisted of a beach, a flat and wide reef section, and a reef face with composite slope.

The reef profile was built from a relatively smooth and impervious plastic material (polyvinyl chloride). The wind generator and wavemaker mechanisms were located at opposite ends of the test flume. Eleven probes (gauges) collected time series surface elevation and wind speed data. Tests were performed without wind (waves-only), with wind-only, and with both waves and wind together. Data obtained in this study will be used in the calibration of numerical models to estimate wave setup and runup affecting the flooding of Pacific islands.

This data report describes the experiment and data. Subsequent reports are expected to address the analyses and use of data and numerical modeling studies. General features of the experiment are summarized in the report, including description of test facility, instrumentation, test conditions, and preliminary results. Raw data are provided on the Coastal Inlets Research Program (CIRP) Web site (*http://cirp.wes.army.mil/cirp/cirp.html*). The analyzed data are presented in Appendix A of this report for each test at nine wave probes, runup gauge and hot-wire anemometer. Values of measured significant wave height, peak wave period, mean water level, and wind speed are provided. The maximum runup, R_{max}, is calculated as maximum vertical excursion of the water level at the shoreline (runup gauge) relative to the still-water level. The runup levels exceeded by 2 percent ($R_{2\%}$) and 10 percent ($R_{10\%}$) of the runup peaks are also tabulated.

Contents

Figures and Tables

Figures

Tables

Preface

This technical report describes design details of a wind-wave flume experiment and data obtained for evaluating numerical wave and surge models for island flooding. The experiment was conducted August-September 2006 jointly by the Surge and Wave Island Modeling Studies (SWIMS) Program and the Coastal Inlets Research Program (CIRP). The main study objectives were to quantify wind effects on wave runup on fringing reefs of the Pacific island of Guam and obtain laboratory data for validation of wave models. Detailed wave measurements were made along a complex reef system consisting of steep slopes and shallow areas for validation of wave breaking, dissipation, wave setup, and wave runup capabilities of the Boussinesq-type wave models and other wave and circulation models. This report is a product of collaborative research by the Surge and Wave Island Modeling Studies (SWIMS) Program and the Coastal Inlets Research Program (CIRP). SWIMS has the lead in this research, with CIRP in a supporting role.

An idealized 1:64 model of a two-dimensional (2-D) fringing reef, representative of the reef systems along the southeast coast of island of Guam, was built in the flume. The reef cross-sectional profile consisted of a beach, a flat and wide reef section, and a reef face with a composite slope. A subsequent report in this series will address validation of the Boussinesq wave model BOUSS-2D with laboratory data and field data obtained for the Pacific islands of Guam and Hawaii.

SWIMS and CIRP are administered by Headquarters, U.S. Army Corps of Engineers (USACE). Research and Development activities of both programs are being conducted at the U.S. Army Engineer Research and Development Center (ERDC), Coastal and Hydraulics Laboratory (CHL), Vicksburg, MS. Program Manager for SWIMS is William Birkemeier, and for CIRP is Dr. Nicholas C. Kraus. The experiment was performed by Dr. Okey G. Nwogu, University of Michigan, and Dr. Zeki Demirbilek and Dr. Donald L. Ward, both Coastal Entrances and Structures Branch (HN-HH), CHL.

Work at CHL was performed under the general supervision of Jose E. Sanchez, Chief of Coastal Entrances and Structures Branch (HN-H);

Unit Conversion Factors

Multiply	By	To Obtain
feet	0.3048	meters
knots	0.5144444	meters per second
miles (nautical)	1,852	meters
miles (U.S. statute)	1,609.347	meters
miles per hour	0.44704	meters per second

1 Introduction

The University of Michigan at Ann Arbor, MI, was contracted by the U.S. Army Engineer Research and Development Center (ERDC), Coastal and Hydraulics Laboratory (CHL), to perform a physical model study at the university's unique wind-wave flume facility. The facility has been used in fundamental research studies of air-sea interaction processes. The goal was to quantify effects of wind on wave and surge processes (wave breaking and dissipation, wave setup, and wave runup) over fringing reefs of the island of Guam. The experiment was performed August-September 2006. The Surge and Wave Island Modeling Studies (SWIMS) is investigating wave propagation over reefs for estimation of wave runup on island shorelines, which was the main objective of this research. The Coastal Inlets Research Program (CIRP) is involved in this study for its responsibility in developing the Boussinesq wave model BOUSS-2D for accurately calculating wave-structure interactions at inlets and navigation projects, which also includes estimating wave setup and runup on structures and shorelines. A subsequent report in this series will provide results from evaluation of both one-dimensional (1-D) and two-dimensional (2-D) Boussinesq models, BOUSS-1D/2D, with laboratory and field data for the Pacific islands of Guam and Hawaii.

The first objective of this study was for SWIMS to investigate the effect of wind on wave processes affecting the inundation of Pacific islands resulting from the passage of typhoons and hurricanes. SWIMS is responsible for developing flood inundation modeling systems for the Pacific islands. The second objective was to obtain laboratory data to evaluate BOUSS-1D/2D model runup calculation capability over steep and highly dissipative slopes and structures, including reef-like surfaces.

Given the prior-stated objectives, the laboratory experiment was designed to investigate potential contribution of wind on wave propagation over fringing reefs. Wave height and period, wave setup, and maximum wave runup values were developed for island flood mapping studies. A representative reef profile for the island of Guam was tested in these experiments. Island flooding and inundation is caused by hurricanes and typhoons and reliable estimates of wave setup and wave runup are required. Site location for the reef in Guam that was replicated in this

laboratory study is shown in Figure 1. Deepwater wave conditions were obtained from Gauge 121 (Figure 1), which is part of the Scripps Institute of Oceanography's field gauging program.

Figure 1. Site of Guam reef and location of offshore wave gauge.

The two images in Figure 2 provide additional information on the reef system and its complex bathymetry. As shown in Figure 3, this reef consists of a wide and flat region, and parts of the flat are dry during low tide. Consequently, the accuracy of measured water levels over the reef flat is crucial in the numerical modeling of waves over these complex reef systems.

It was necessary to perform a laboratory study in a combined wind and wave setting to quantify wind effects entering into estimates of wave processes over reefs (i.e., wave setup and runup) for the island flooding and inundation planning studies. To achieve this objective, a fringing reef

geometry representative of reef systems off the southeast coast of Guam was built. This reef model was placed in a wind-wave flume and tested for both typical and extreme wave and wind conditions as observed at the site. Details of the laboratory experiment and data are described in the subsequent chapters of this report.
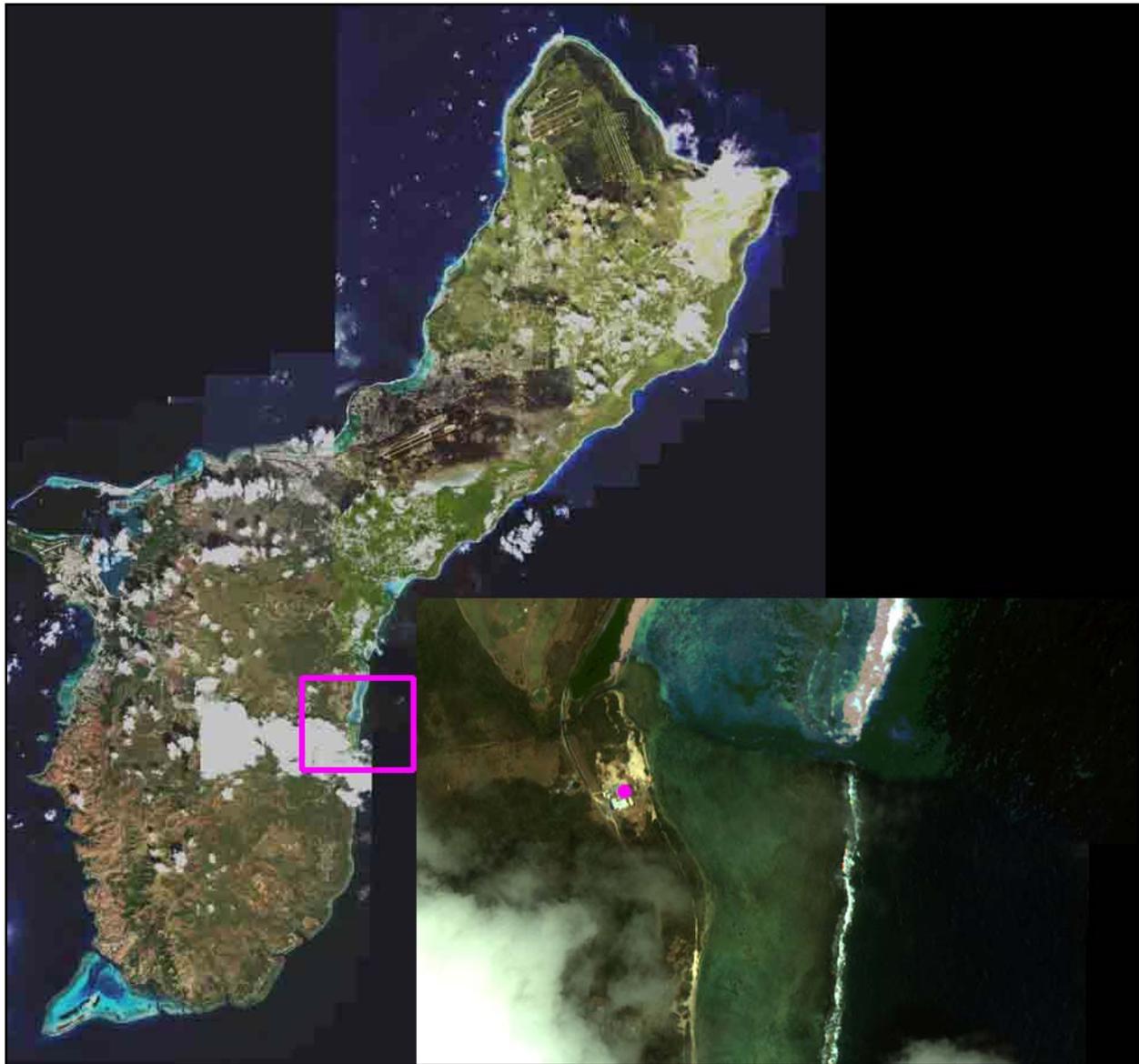
Figure 2. Images of Guam reef and bathymetry.

Figure 3. Guam reef during low tide.

2   Details of Experiment

Description of facility

The experiment was conducted at the University of Michigan wind-wave facility. The flume is 35 m long, 0.7 m wide, and 1.6 m high. Figures 4 and 5 are photographs of the facility. A computer-controlled, non-absorbing plunger-type wavemaker is installed at one end of the flume (Figure 6). The wavemaker can generate irregular sea states with significant wave heights up to 10 cm and wave frequencies from 0.4-10 Hz. Wind is generated in the facility using an open loop suck-down apparatus, in which a blower is positioned at the downstream end of the flume that sucks air from an intake tunnel located at the upstream end of the facility near the wavemaker. The test section between the entrance tunnel and blower is sealed with a glass top. The 40-horsepower (29.8-kW) blower is capable of producing winds up to 30 m/sec.
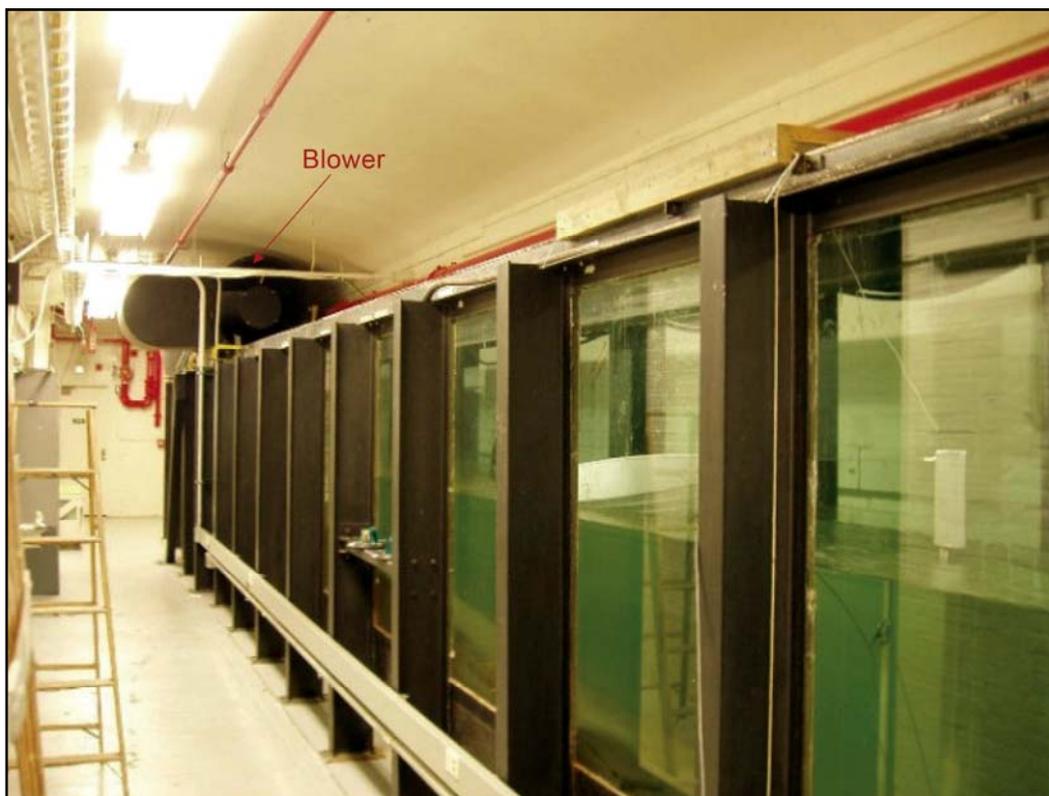
Figure 4. Side view of wind-wave flume from the wavemaker end.

Figure 5. Wind-wave flume during instrument calibration.

Figure 6. Wedge wavemaker used to generate waves.

Experiment design

An idealized 1:64 model of 2-D fringing reef was built in the flume. It was a 2-D vertical model, uniform across the tank width that was placed in cross-shore along the flume length. The model was vertical and cross-shore, but uniform across the tank width. The layout of wind-wave flume and experiment design is depicted in Figure 7a. Geometry of the cross-sectional profile of the reef-beach system is shown in Figure 7b. The profile consists of a 1:12 beach followed by a 4.8-m-wide reef flat and a composite slope reef face. The cross section of the reef face is similar to the one used in previous hydraulic model tests by Seelig (1983). However, a flat reef top was placed in these experiments instead of the lagoon in Seelig (1983). The flat reef top is more typical of conditions along the southeast coast of Guam. The reef surface was built using polyvinyl chloride (PVC), a relatively smooth and impervious material. The toe of the reef slope was located approximately 15.7 m from the wavemaker.

Instrumentation

Nine capacitance-wire wave gauges measured the water-surface elevation in the flume (Figure 7b). Six of the gauges were positioned over the reef structure, and the remaining three gauges were installed in the constant-depth section of the flume to quantify the amount of wave reflection from the reef face. Wave Gauges 1–6 were capacitance-type wave gauges built at ERDC/CHL. Gauges 7–9 were capacitance-type wave gauges manufactured at the University of Michigan.

The wave probes located seaward of the reef were arranged in a three-gauge array to allow separation of the incident and reflected wave trains (Figure 7b). The wave probes over the reef flat were designed to provide accurate measurements of wave setup over the reef flat. The bottom ends of the probes were inserted into holes drilled into the reef surface, allowing the probes to record water-level changes over the reef flat from an initially dry reef surface.

a. Layout.

b. Reef profile geometry and gauge locations

Figure 7. Wind-wave flume.

A 1-m-long capacitance-wire runup gauge (Gauge Model WG-50 manufactured by RBR, Ltd.) was installed on the beach (Figure 8). This runup gauge was placed at either of two positions, depending on the still-water level. The lower end of the runup gauge was approximately 2.01 cm above reef flat for the lower water-level tests, and 4.83 cm above the reef flat for the higher water-level tests. All wave gauges were calibrated at the same time by filling the tank to five different water levels and fitting a first-order polynomial to the measured voltages. The maximum relative error over the calibration range (12 cm) was 0.4 percent for Gauges 1–6, 0.6 percent for Gauges 7–9 and 0.4 percent for the runup gauge.

Figure 8. Runup gauge at downstream end of wind-wave flume.

Two anemometers measured the wind speed in the flume. A cup-style anemometer (Figure 9) was installed near the air intake, and a hot-wire anemometer was installed over the reef flat. The cup anemometer was an Oregon Scientific Electronic Weather Station Model WM918 with an advertised accuracy of 0.18 m/sec or 0.4 mph. The hot-wire anemometer (Air Velocity Transducer Model 8455-09) was built by TSI, Inc. and has an accuracy of 0.1 m/sec. The cup anemometer did not have digital recording capability and was primarily used during the calibration of the wind speeds.

Figure 9. Cup-style anemometer.

Coordinates of gauges and hot-wire anemometer are listed in Table 1, in which (0,0) is toe of slope, and positive values are upwards (vertical) and towards slope (horizontal).

Table 1. Gauge coordinates.

Sensor	X (m)	Z (m)
Gauge 1	-1.11	0
Gauge 2	-0.92	0
Gauge 3	-0.59	0
Gauge 4	2.75	0.33
Gauge 5	3.68	0.39
Gauge 6	4.22	0.45
Gauge 7	4.8	0.5
Gauge 8	6.97	0.5
Gauge 9	9.14	0.5
Hot-wire anemometer	7.5	1.35

Test conditions

Approximately 80 tests were conducted for different combinations of wave-only, wind-only, and combined wind-wave tests. The wave-only test conditions are summarized in Table 2. The significant wave height H_s and spectral peak period T_p were obtained from a spectral analysis of the recorded time series data at the middle gauge of the offshore array (Gauge 2). The table is sorted by the spectral peak period values, and consequently test numbers may not appear in increasing order. The wind-only test conditions are listed in Table 3. The combined wind and wave test conditions are also sorted by the spectral peak period values and summarized in Table 4. The H_s and T_p for the combined wind-wave conditions were in general larger than those for the wave-only test conditions due to the contribution of the wind-generated waves.

The tests at laboratory-scale (1:64) consisted of irregular sea states with significant wave heights ranging from 3 to 8.5 cm, spectral peak periods ranging from 1 to 2.5 sec, and water levels ranging from 50 to 55 cm above the flume floor or still-water depths h_r of 0 to 5 cm on reef flat. The 50-cm water depth corresponds to an initially dry reef flat, similar to a reef flat exposed at low tide as shown in Figure 3. Time-histories of the water surface elevation were synthesized from Joint North Sea Wave Analysis Project (JONSWAP) spectral shapes with peak enhancement factor γ = 3.3 using the random phase method. Linear theory was used to convert the water surface elevation to control signals for the wavemaker.

All gauges were sampled for 15 min at 20 Hz. The gauges were zeroed before each test to minimize drift. Data collection was initiated shortly after the wavemaker was started with initially calm water conditions.

Table 2. Summary of wave-only test conditions.

Test Number and Data File	H_s (cm)	T_p (sec)	h_r (cm)	Wind Speed (m/sec)
Test 15.dat	6.2	1.00	5.1	0.1
Test 20.dat	6.1	1.25	5.1	0.0
Test 16.dat	5.2	1.50	5.1	0.1
Test 17.dat	7.8	1.50	5.1	0.1
Test 21.dat	8.2	1.75	5.1	0.1
Test 18.dat	8.5	2.00	5.1	0.1
Test 19.dat	8.3	2.50	5.1	0.1
Test 26.dat	5.8	1.00	1.6	0.1
Test 27.dat	5.5	1.25	1.6	0.0
Test 28.dat	4.7	1.50	1.6	0.1
Test 29.dat	7.1	1.50	1.6	0.0
Test 30.dat	7.6	1.75	1.6	0.1
Test 31.dat	8.5	2.00	1.6	0.1
Test 32.dat	7.9	2.50	1.6	0.0
Test 33.dat	5.6	1.00	0.0	0.1
Test 34.dat	4.5	1.50	0.0	0.0
Test 35.dat	4.5	1.50	0.0	0.0
Test 36.dat	6.8	1.50	0.0	0.0
Test 37.dat	7.6	1.75	0.0	0.0
Test 38.dat	8.4	2.00	0.0	0.0
Test 39.dat	7.7	2.50	0.0	0.0
Test 44.dat	3.2	1.00	3.1	0.0
Test 45.dat	6.1	1.00	3.1	0.1
Test 46.dat	5.9	1.25	3.1	0.1
Test 47.dat	5.0	1.50	3.1	0.1
Test 48.dat	7.5	1.50	3.1	0.1
Test 57.dat	7.7	1.75	3.1	0.1
Test 58.dat	8.5	2.00	3.1	0.1
Test 59.dat	8.2	2.50	3.1	0.0

Table 3. Summary of wind-only test conditions.

Test Number and Data File	h_r (cm)	Wind Speed (m/sec)	Wind Gust (m/sec)
Wind cal U1.dat	3.1	1.0	0.05
Wind cal U2.dat	3.1	2.0	0.08
Wind cal U3.dat	3.1	3.1	0.11
Wind cal U4.dat	3.1	4.0	0.14
Wind cal U5.dat	3.1	4.7	0.16
Wind cal U6.dat	3.1	5.4	0.18
Wind cal U7.dat	3.1	6.3	0.20
Wind cal4 U3.dat	3.1	2.7	0.25
Wind cal4 U6.dat	3.1	4.6	0.26
Wind cal4 U8.dat	3.1	5.9	0.32

Table 4. Summary of combined wind-wave test conditions.

Test Number and Data File	H_s (cm)	T_p (sec)	h_r (cm)	Wind Speed (m/sec)
Test 67.dat	3.2	1.00	3.1	3.1
Test 66.dat	6.0	1.00	3.1	3.1
Test 65.dat	5.8	1.25	3.1	3.1
Test 64.dat	4.9	1.50	3.1	3.1
Test 63.dat	7.4	1.50	3.1	3.2
Test 62.dat	7.7	1.75	3.1	3.2
Test 61.dat	8.5	2.00	3.1	3.2
Test 60.dat	8.1	2.50	3.1	3.2
Test 75b.dat	3.4	1.00	3.1	4.2
Test 74b.dat	6.2	1.00	3.1	4.5
Test 73b.dat	6.0	1.25	3.1	4.8
Test 72b.dat	5.1	1.50	3.1	4.4
Test 71b.dat	7.5	1.50	3.1	5.2
Test 70b.dat	7.8	1.75	3.1	5.3
Test 69b.dat	8.5	2.00	3.1	5.5
Test 68.dat	8.1	2.50	3.1	5.5
Test 83b.dat	2.9	1.00	0.0	1.6
Test 82b.dat	5.6	1.00	0.0	1.4
Test 81b.dat	5.1	1.25	0.0	1.8
Test 80b.dat	4.4	1.50	0.0	1.8
Test 79b.dat	6.7	1.50	0.0	2.0
Test 78b.dat	7.5	1.75	0.0	2.1
Test 77b.dat	8.3	2.00	0.0	2.1
Test 76b.dat	7.6	2.50	0.0	1.9

Test Number and Data File	H_s (cm)	T_p (sec)	h_r (cm)	Wind Speed (m/sec)
Test 92.dat	3.1	1.00	0.0	5.3
Test 91.dat	5.7	1.00	0.0	5.3
Test 90.dat	5.3	1.25	0.0	3.7
Test 89.dat	4.5	1.50	0.0	3.7
Test 88.dat	6.8	1.50	0.0	4.0
Test 87.dat	7.5	1.75	0.0	3.8
Test 85.dat	8.2	2.00	0.0	5.3
Test 84.dat	7.6	2.50	0.0	5.4
Test 101.dat	3.3	1.00	0.0	5.3
Test 100.dat	6.0	1.00	0.0	6.9
Test 99.dat	5.5	1.25	0.0	7.1
Test 98.dat	4.7	1.50	0.0	7.1
Test 97.dat	7.0	1.50	0.0	7.1
Test 96.dat	7.6	1.75	0.0	5.4
Test 95.dat	8.3	2.00	0.0	5.6
Test 94.dat	7.6	2.50	0.0	5.4
Test 109.dat	3.8	1.00	3.1	6.5
Test 108.dat	6.6	1.00	3.1	6.7
Test 107.dat	6.3	1.25	3.1	6.8
Test 106.dat	5.4	1.50	3.1	6.7
Test 105.dat	7.8	1.50	3.1	6.0
Test 104.dat	8.0	1.75	3.1	5.8
Test 103.dat	8.6	2.00	3.1	7.1
Test 102.dat	8.2	2.50	3.1	7.0

3 Results and Discussion

Description of raw data files

Raw data collected in the experiment are posted on the Coastal Inlets Research Program (CIRP) Web site (*http://cirp.wes.army.mil/cirp/cirp. html*) for downloading. Each test has its own file containing data from 11 probes (wave Gauges 1 to 9, runup gauge, and hot-film anemometer).

Each data file has a header section, which is followed by a data section. A sample data file is shown as follows:

```
Channels        11
Samples      18000
Frequency       20
Gains
    0.252     0.309      0.266     0.375      0.327     0.239      0.1265    0.1299     0.117     0.9386          1
Offsets
-0.191051  3.517864  5.331282 -4.992504   -6.59183 -5.723676 -1.871649 -1.189118 -1.099374  1.681036   0.015758
Wave1;    Wave2;    Wave3;    Wave4;    Wave5;    Wave6;    Wave7;    Wave8;    Wave9;    Runup;    Wind1;
 0.113878   0.08559  -0.16698  0.063019 -0.005499 -0.004673 -4.011867  0.010578  0.006332  -0.00989 -0.000499
 0.129621   0.10238  0.095746  0.036977  0.102759  0.019587 -10.95492 -0.034059  0.155007 -0.003062  0.000111
-0.052031  0.124107  0.044119  0.020701 -0.011099  0.047679 -9.181762 -0.085744 -0.051052  0.003766  0.000417
 0.147786  0.081639  0.081979  0.016632 -0.002699  0.032356  0.033823  0.092804  0.074149  0.003441  0.000722
 0.196227  0.104355  0.085421  0.047557 -0.094159  0.038741 -0.091625  0.027023 -0.035402 -0.001111  0.002553
 0.150208  0.154724  0.001669  0.059764  0.035564  0.036187 -0.057851  0.052865  0.019373  0.017422 -0.001414
 0.209548  0.132996  0.182939   0.03535 -0.001766  0.059171  -0.11575  0.062263  0.037632 -0.003062  0.006215
 0.150208   0.32262  0.141637  0.014191 -0.011099  0.027249  0.009698  0.012927 -0.051052 -0.008264  -0.00172
 0.130832  0.149786  0.141637  0.045929   0.04023  0.018311 -0.132637 -0.052854 -0.030185  0.004416  0.001332
 0.061804  0.157686  0.125575   0.02477  0.020632  0.121738 -0.130224 -0.219655  0.105449  0.035955  0.000111
 0.089657  0.133984  0.172614  0.028839  0.013166  0.185583 -0.004777  0.043468  0.021982  0.011894  0.005605
```

The header section in each data file contains information about the number of data acquisition channels (11), number of data points in each record (18,000), sampling frequency (20 Hz) and the values of the calibration gains (cm/volt) and offsets (volts). The data section contains 11 columns of data. Columns 1–9 represent the measured water-surface elevation at Gauges 1–9 respectively in centimeters, column 10 represents the runup elevation time-history in centimeters, and column 11 represents the direct anemometer output in volts. The wind speed conversion factor for the anemometer output is 1.25 m/sec per volt.

Preliminary data analysis

The measured time-histories were analyzed to extract engineering quantities of interest. This section presents a brief description of two types of analyses applied to the raw data. Next, results from these analyses are examined. The preliminary analyses performed illustrate types of analyses users could apply to the raw data to determine data trends. Users may use sample results for comparison of their own analyses of raw data. Two types of analyses were performed, a reflection analysis for three offshore gauges, Gauges 1–3, and a statistical and spectral analysis for Gauges 1–9. After a short description of these analyses, results are discussed in detail.

Reflection analysis

The measured time-histories at the three offshore probes, Gauges 1–3, located in the constant water depth offshore of the reef face, were analyzed by the least-squares method of Mansard and Funke (1980). The analysis was performed over the incident wave energy band (0.25 Hz to 1.5 Hz) to estimate the wave reflection coefficient.

The results of the reflection analysis are summarized in Table 5. The value of calculated reflection coefficient R is in percent (i.e., $R = 4.3$ percent for $H_s = 6$ cm, $T_p = 1$ sec, and water level = 50.0 cm). The calculated values of reflection coefficients were all less than 10 percent. These values are consistent with previous reef reflection coefficient estimates by Massel and Gourlay (2000).

Table 5. Calculated wave reflection coefficients.

Target H_s (cm)	Target T_p (sec)	Wave Reflection Coefficients (%)			
		h_r =0.0 cm	h_r =1.6 cm	h_r =3.1 cm	h_r =5.1 cm
6	1	4.3	4.3	4.3	3.9
6	1.25	–	5.7	5.2	5.4
5	1.5	5.9	5.7	5.0	5.3
8	1.5	5.7	5.6	5.3	5.1
8	1.75	8.2	7.7	7.4	6.6
8	2	9.2	9.6	8.9	7.6
8	2.5	8.9	9.0	9.1	7.7

Note that long waves (0 to 0.25 Hz) were also observed at the offshore gauge locations. These waves could be bound waves due to nonlinear wave

effects in shallow water (e.g., Longuet-Higgins and Stewart 1964), offshore propagating waves generated at the wave breaking location (Symonds et al. 1982), or long-waves reflected from the shoreline. Long waves are difficult to absorb even with active absorption wavemakers. Hence, data collection was initiated from calm water conditions to aid in interpretation of the results.

Statistical and spectral analysis

In this analysis, spectral densities of the water-surface elevation time-histories were obtained by Fourier transforming the raw data and band-averaging over 31 frequency components, resulting in 62 deg of freedom (dof) with a frequency resolution of 0.019 Hz. Data analysis began 100 sec after the start of data collection to allow waves to reach the gauges and establish steady-state conditions. The total record length analyzed was 800 sec. The significant wave height is calculated as:

$$H_s = 4\sqrt{m_0}$$

where m_0 is the zeroth moment of the water surface spectrum,

$$m_0 = \int_0^{f_{ny}} S(f)df$$

where f_{ny} is the Nyquist frequency and $S(f)$ is the spectra density as a function of frequency, f. The peak period is the inverse of the frequency with the maximum energy density.

The mean water level at each gauge was calculated directly from the time records. Runup statistics were also obtained by analyzing time series data from the runup gauge. The maximum runup (R_{max}) is calculated as maximum vertical excursion of the water level at the shoreline (runup gauge) relative to the still-water level. The runup level exceeded by 2 and 10 percent ($R_{2\%}$ and $R_{10\%}$) of the runup peaks were also calculated.

The summary results from the preliminary analysis of raw data are provided in tables in the appendix. For each test, values of the significant wave height, peak wave period, and mean water level are calculated at the probe locations. The values of R_{max}, $R_{2\%}$, $R_{10\%}$, and wind speed are also given at the end of each table. The analyzed results are all in laboratory scale (i.e., H_s, $\bar{\eta}$, R_{max}, $R_{2\%}$, $R_{10\%}$ are in centimeters, T_p is in seconds, and

wind speed values in meters per second). The calculated results with a significant drift over the 900-sec (15-min) test time have been eliminated from the tables in the appendix (entries with "-").

The model scale factor (1:64) and Froude scaling may be used to convert the analyzed data results in the tables in the appendix to equivalent prototype conditions. By Froude scaling, the velocity and period scale factor would be 1:8, and the length scale is 64. For example, Test 61 prototype conditions would be H_{mo} = 5.5 m, T_p = 16 sec, and with Froude scaling the prototype wind U=24 m/sec. Scaling of wind speed values is more complicated due to the Reynolds number dependence of the shear stress (drag) coefficient and possible differences in the structure of the air-water boundary layer between model and prototype as discussed in (Jeffreys 1924; Miles 1957; Wu 1969; Banner 1990; Young 1999; and Donelan et al. 2006). For coastal wave surge modeling, Demirbilek et al. (1993) provide specific guidance, including computing methods and examples, for estimation of the wind shear stress drag coefficients as a function of wind speed.

Analysis results for wave-only tests

Figures 10 to 12 show plunging breaking waves observed during Test 18. These photographs were taken in the vicinity of Gauge 6 (Figure 7), which was located just shoreward of the reef crest. After breaking, the waves reformed as bores and propagated across the reef flats toward the beach. Several types of bores were observed during the tests ranging from undular bores (without visible breaking at its front) to fully turbulent bores with turbulent roller regions in the front.

These bores evolved significantly as they traveled over the flat reef section. Because bore propagation speed is related to bore height, larger bores propagated faster and captured smaller bores. In a number of tests, offshore propagating bores were also observed. These offshore propagating bores occurred more frequently when turbulent bores were generated on the reef flat. Turbulent bores transported a bulk of water in the roller region that led to a buildup of the mean water level at the shoreline. During a lull between groups of high waves, the piled-up water was released as an offshore propagating bore.

Figure 10. Initial plunging breaking waves for Test 18 near the reef crest.
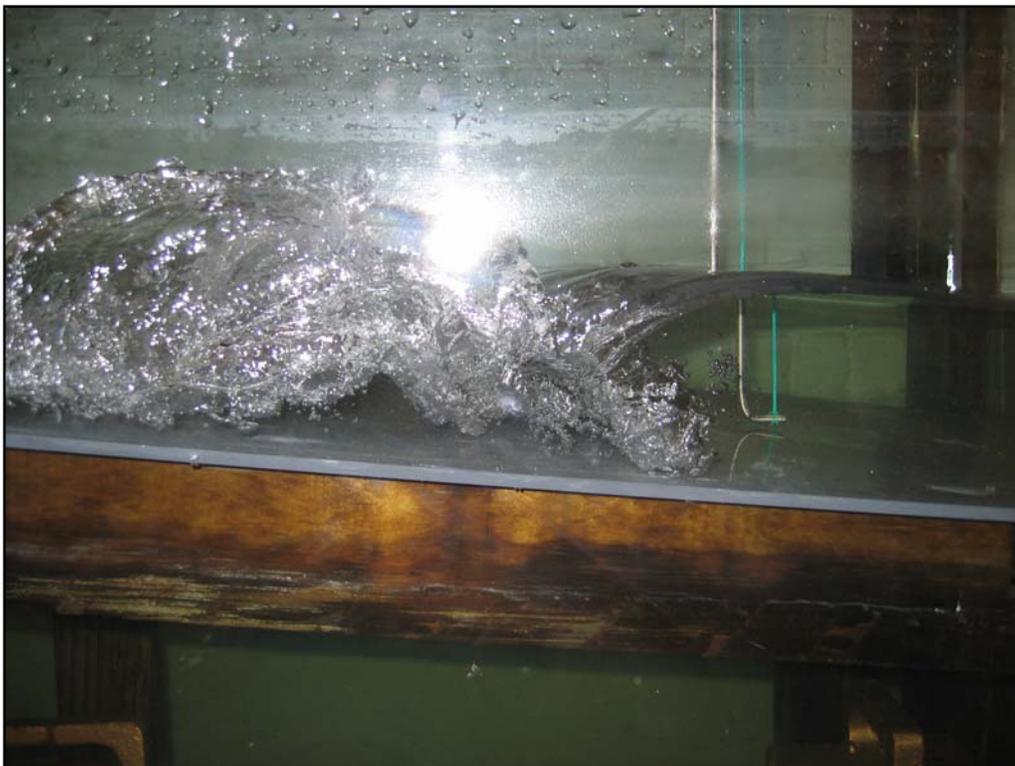
Figure 11. Middle plunging breaking waves for Test 18 near the reef crest.

Figure 12. Final plunging breaking waves for Test 18 near the reef crest.

Sample time series data at Gauges 7–9 on the reef flat and the runup gauge are shown in Figure 13 for Test 48. The waves underwent a significant evolution over the reef flat with an increase in the long-period wave energy as the waves propagated shoreward.

Figure 14 shows wave energy spectra from offshore Gauge 2, an intermediate gauge on the reef face (Gauge 5), and the most landward gauge on the reef face (Gauge 6). As the waves propagated over the reef face into shallower water, energy was transferred from the peak of the spectrum to lower and higher frequencies. The spectral densities of the reef flat Gauges 7–9 are shown in Figure 15.

Wave breaking occurred both on the reef face and reef crest. After breaking, there is still a considerable amount of wave energy around the peak frequency of the incident wave spectrum (f_p = 0.67 Hz) at the reef crest (Gauge 7). However, the spectrum of the gauge located at the middle of the reef flat (Gauge 8) is dominated by low-frequency energy with most of the wave energy around the incident peak frequency dissipated. The low-frequency energy grows as the waves propagate shoreward as shown in the spectrum of the gauge at the toe of the beach (Gauge 9).
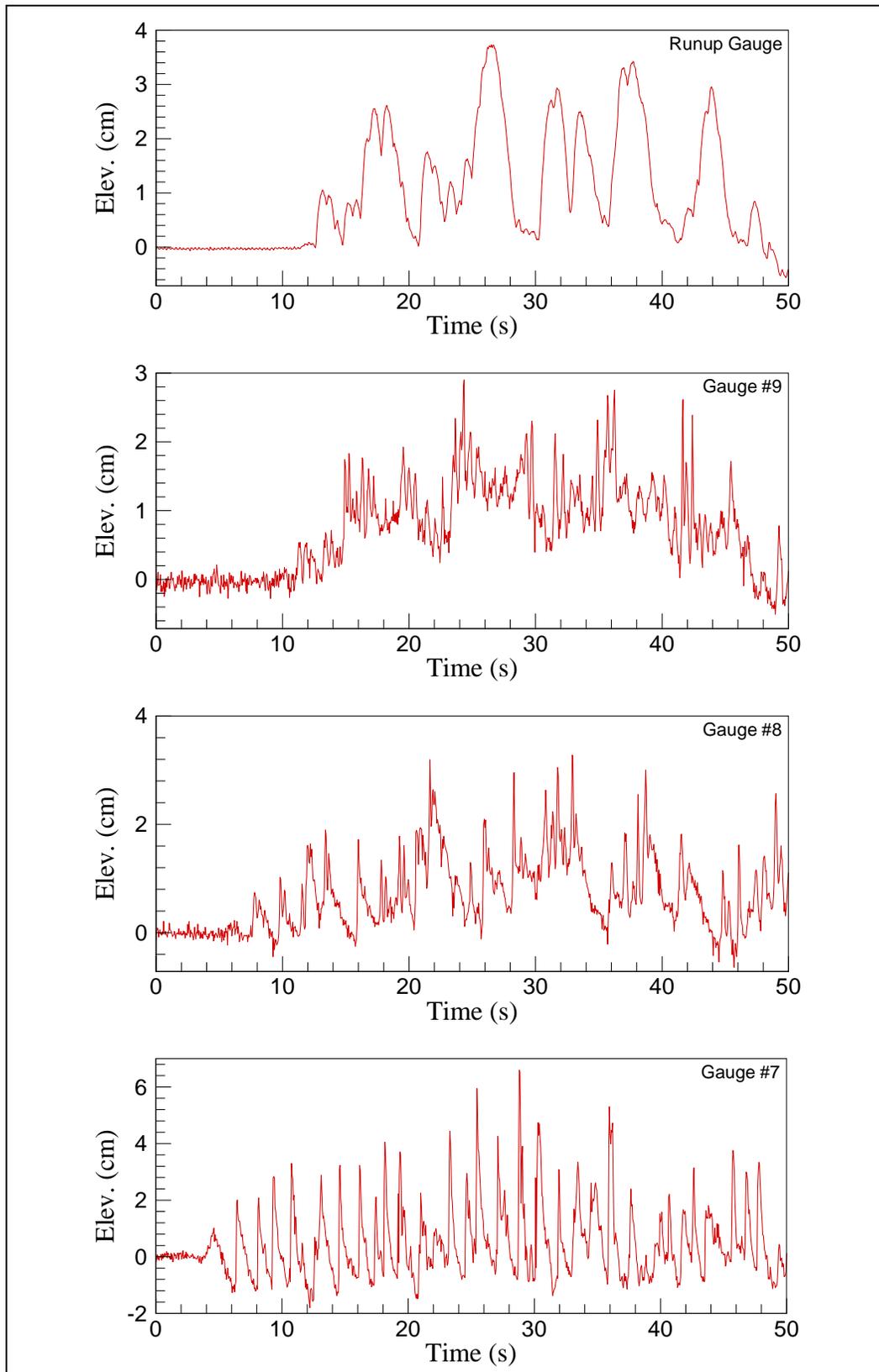
Figure 13. Time series samples for Test 48 at runup gauge and Gauges 7-9.
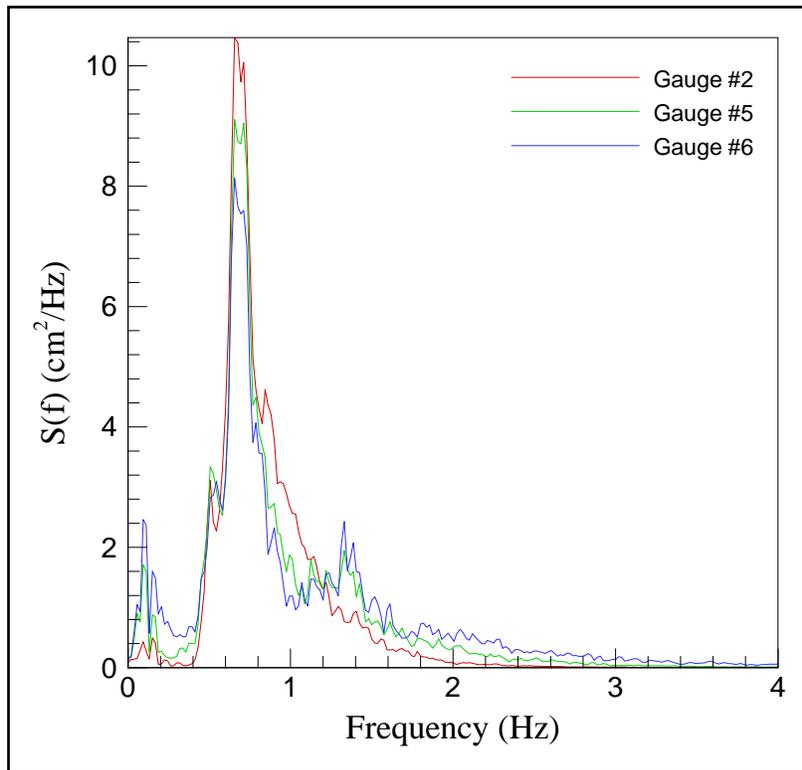
Figure 14. Wave energy spectra for Test 48 at Gauges 2, 5, and 6.
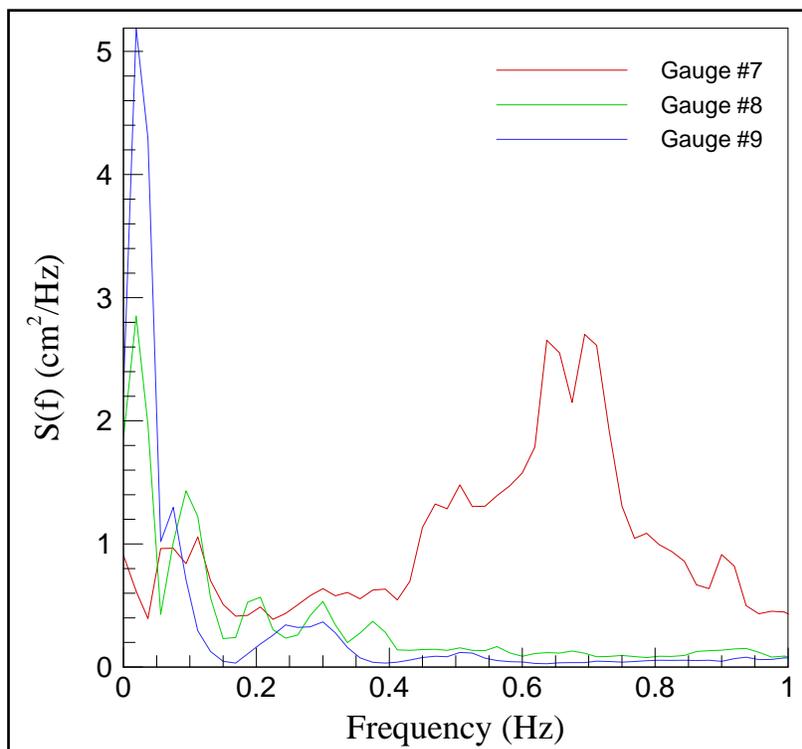
Figure 15. Wave energy spectra for Test 48 at Gauges 7–9.

The nonlinear evolution of the spectrum over the reef flat was further investigated by reanalyzing the spectral densities at a finer frequency resolution of 0.0025 Hz corresponding to 10 dof. Figure 16 shows a detailed view of the spectrum in the low frequency region (0–0.25 Hz). Gauges 8 and 9 located at the middle and landward end of the reef flat, respectively, had spectral peak periods of approximately 35 sec. There is, however, little energy at the 35-sec period at reef crest Gauge 7. The reef-beach system can be considered to be an open basin with natural oscillation periods given by:

$$T_n = \frac{4l_r}{(2n-1)\sqrt{g(h_r + \bar{\eta})}}$$

where l_r = 4.8 m is the width of the reef top and h_r is still-water depth over the reef flat. The 35-sec period corresponds to the first reef oscillation mode (n = 1) with a wavelength approximately equal to four times the width of the reef flat. The first mode has a node at the reef crest and an anti-node at the shoreline. The trapped waves would thus be resonantly amplified at the shoreline relative to the incident energy at the reef crest.
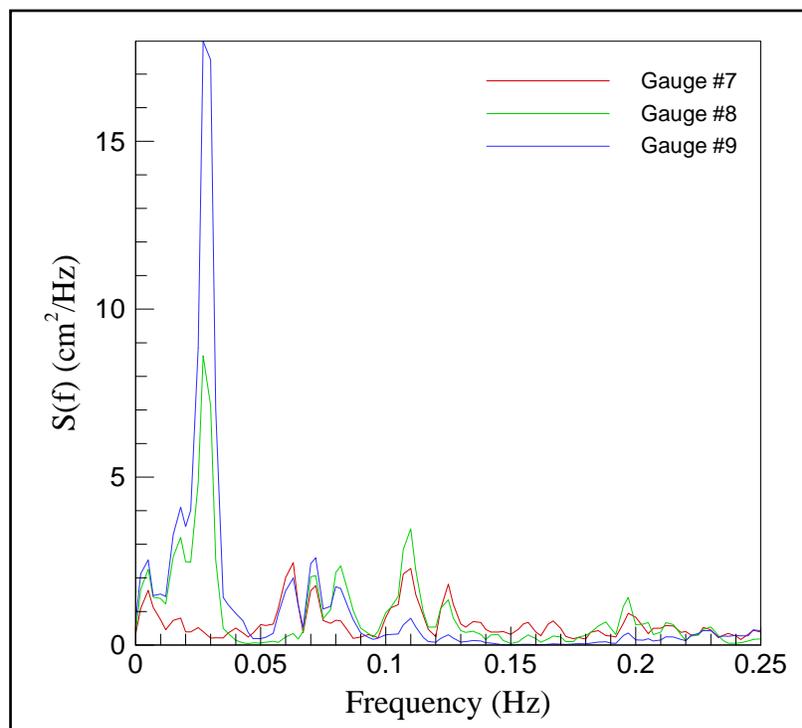
Figure 16. Low-frequency wave energy spectra for Test 48 at Gauges 7–9.

Next, the overall trends in the data were analyzed. The mean water-level setup on the reef flat and runup on the beach face depend primarily on the significant wave height, H_s, and spectral peak period, T_p, of the incident waves, and the still-water depth over the reef flat h_r. The nondimensional water-level setup at Gauge 9 at different water levels is plotted against the deepwater incident wave power parameter $H_{mo}^2 T_p$ in Figure 17. See also Seelig (1983) for runup predictions versus this parameter.
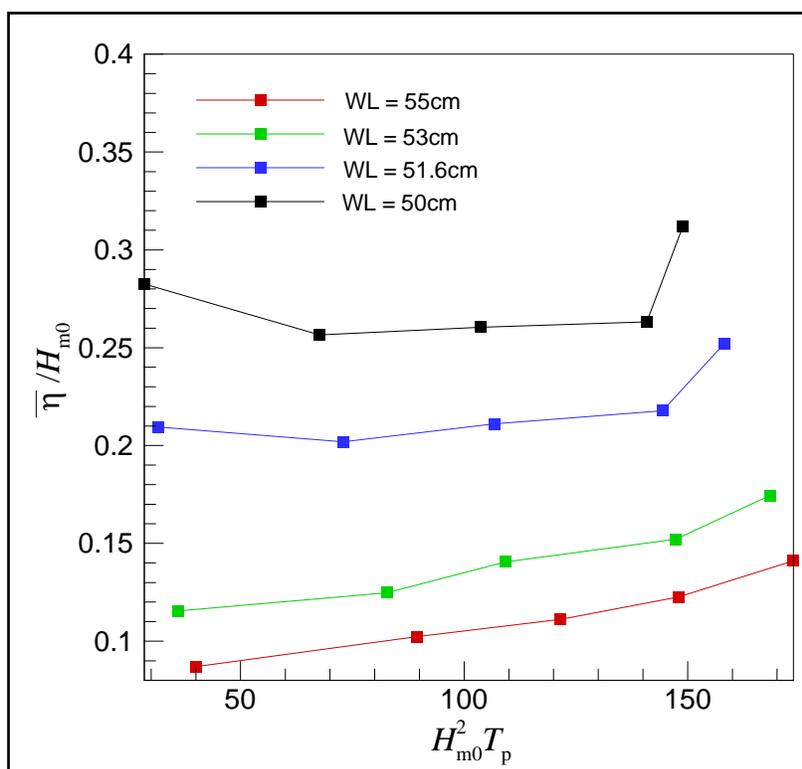
Figure 17. Wave setup versus wave power for Test 48 at Gauge 9 for different water levels.

The wave setup increased with decreasing water level on the reef flat. This trend has also been reported by other investigators (Seelig 1983; Gourlay 1996; Massel and Gourlay 2000). The wave setup also increased with increasing values of the wave power ($H_{mo}^2 T_p$) at the higher water levels (h_r = 3 cm and 5 cm) similar to previous observations by Seelig (1983) for the lagoon case. At lower water levels (h_r = 0 cm and 1.6 cm), the wave setup was relatively independent of $H_{mo}^2 T_p$. This represents a major difference between reef-lagoon type bathymetry used in the Seelig experiments and the flat reef top bathymetry used in these experiments.

The nondimensional maximum wave runup values are plotted against the incident wave power $H_{mo}^2 T_p$ in Figure 18. In general, the maximum runup values increased with increasing $H_{mo}^2 T_p$ values. There appeared to be little difference in the nondimensional runup values for the different water levels. There is, however, more variability at lower values of $H_{mo}^2 T_p$ corresponding to shorter period (T_p = 1-sec and 1.25-sec) waves. This might be due to a transition in the nature of the runup process from trapped infragravity modes at the longer periods to individual wave runup events at shorter periods.
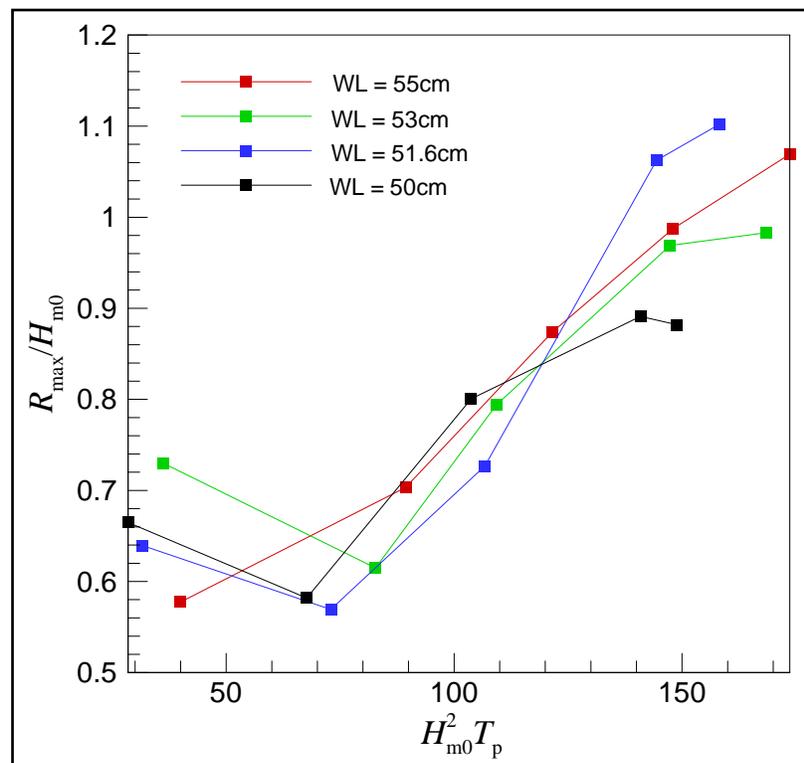
Figure 18. Maximum runup versus wave power for different water levels.

Analysis results for wind-only tests

The wind-only test data were analyzed to investigate the spectral properties of the short-period gravity capillary waves generated by the wind as well as the wind-induced setup and runup over the reef. Figure 19 shows the spectral densities from Gauges 2, 6, and 9 for the Wind-Cal4-U8 test condition (U = 5.8 m/sec). The significant height of short-period wind-generated waves grew with increasing distance (fetch) from the air intake. For the test condition shown in Figure 19, the significant wave height increased from 2 cm at Gauge 2 to 3.1 cm at Gauge 6. The peak

spectral period also increased from 0.3 sec at Gauge 2 to 0.43 sec at Gauge 6. The 3-cm water depth over the reef flat limited further wave growth, but the spectral peak period increased from 0.43 sec at Gauge 6 to 0.5 sec at Gauge 9.
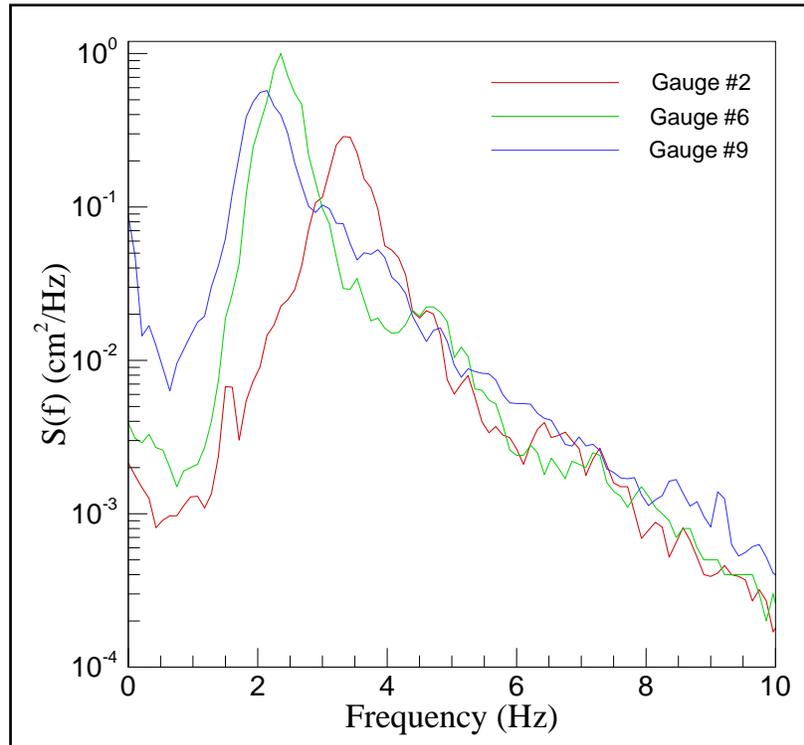
Figure 19. Variation of wave spectra from offshore Gauges 2 to mid-reef Gauge 6 to beach toe Gauge 9 for Test Wind-cal4-U8.

The wind-induced setup values over the reef flat are plotted in Figure 20 for three different wind speeds. The wind setup increases with increasing fetch distance and wind speed. The mean water level at the runup gauge was, however, always consistently less than that at the toe of the beach. This can be explained by examination of the time and depth-averaged momentum equation as follows. The shear stress applied by the wind at the water surface τ_s is balanced by the bottom shear stress τ_b and gradients of the velocity head $u^2/2g$ and atmospheric pressure p_{atm}:

$$\frac{\partial \eta}{\partial x} = \frac{1}{g}\left[\frac{\tau_s - \tau_b}{\rho g (h+\eta)} - \frac{\partial}{\partial x}\left(\frac{\bar{u}^2}{2} + \frac{p_{atm}}{\rho}\right)\right]$$
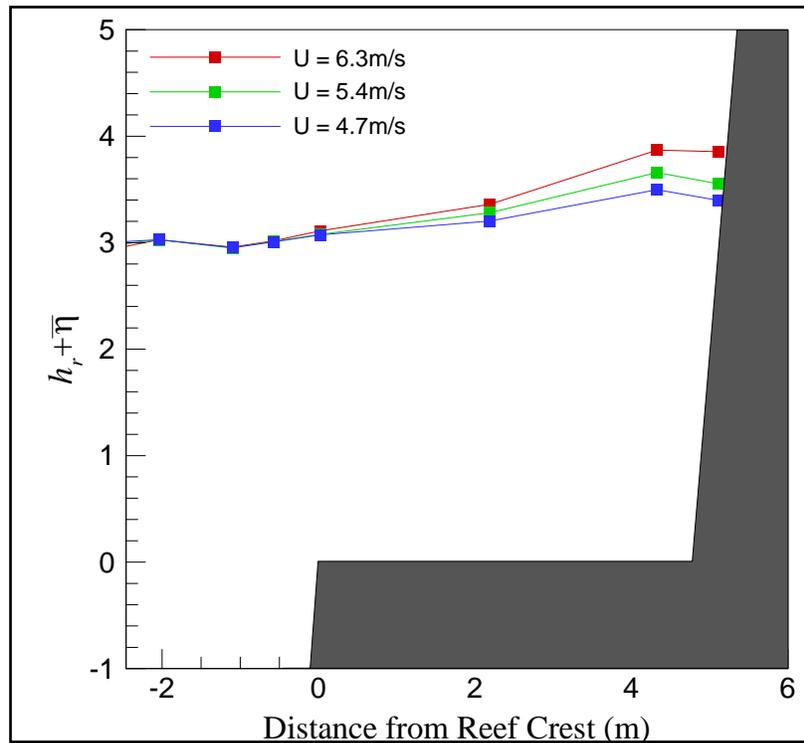
Figure 20. Variation of wind setup plus water depth over reef flat for three wind speeds.

Assuming that the atmospheric pressure remained approximately constant as the air flows over the beach, the reduction in water level at the shoreline could be attributed to changes in the velocity head as the wind-induced surge propagates up the beach. The wind-induced current may not be depth-uniform because the wind shear stress generates a surface current in the direction of the wind while the wind-induced setup induces an opposing current (Jeffreys 1924; Miles 1957; Banner 1990; Massel and Gourlay 2000).

Next, the variation of the wind-induced setup at the mid-reef top Gauge 8 and beach toe Gauge 9 was investigated (Figure 21). Because the wind shear stress is often parameterized using the quadratic drag law $\tau_s = \rho_{air} c U^2$, the wind speed was plotted against depth-based Froude number U^2/gh_r. The overall trend appears to be linear, supporting the quadratic shear stress hypothesis (Jeffreys 1924; Miles 1957; Demirbilek et al. 1993; Young 1999; Donelan et al. 2006).
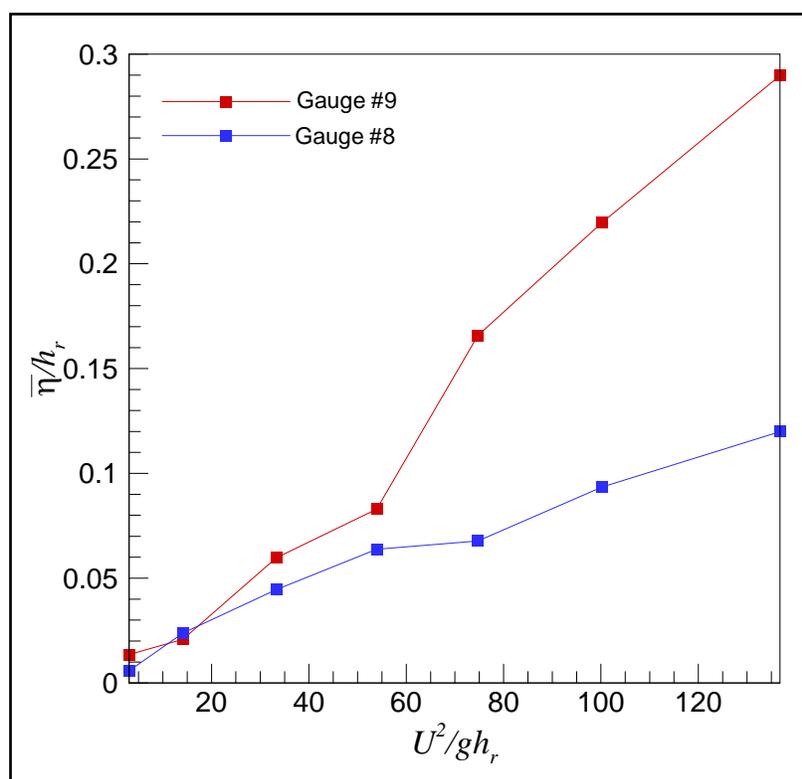
Figure 21. Wind-induced setup variation with wind speed at Gauges 8 and 9.

Analysis results for combined wind-wave tests

The effect of wind on the mechanically-generated waves can be seen in Figures 22–24 where the spectral densities at Gauges 2, 7, and 9 are plotted for different wind speeds. Prior to wave breaking, the wind-generated surface ripples enhance the high-frequency tail of the spectrum as shown in Figure 22 for offshore Gauge 2. Wave breaking, however, leads to the dissipation of the high-frequency energy. The spectral densities at Gauge 7, which is located at the reef crest just beyond the predominant breaking location, are similar for the wave-only/wave-wind cases. After breaking, the wind starts anew to transfer momentum to the waves and enhance the high-frequency tail of the spectrum over the reef flats as seen in Figure 24 for Gauge 9.

The wind also enhanced the low-frequency trapped oscillations near the shoreline (Symonds et al. 1982; Seelig 1983; Gourlay 1996; Massel and Gourlay 2000). Figure 25 shows the higher resolution (10 dof) spectral densities over the low-frequency region (0–0.25 Hz). The wind-induced enhancement of the low-frequency oscillations was not a consistent function of wind speed. The intermediate wind speed $U = 3$ m/sec excited

a larger trapped mode than the greater wind speed U = 6 m/sec. This seems to suggest that the enhancement might depend on details of the air-sea boundary layer. It should also be pointed out that although the wind increased the low-frequency energy near the shoreline, the low-frequency energy at mid-reef flat Gauge 8 decreased slightly as shown in Figure 26.

Nondimensional water-level setup values at Gauges 8 and 9 are plotted as a function of wind speed in Figures 27 and 28, respectively, for test conditions with h_r = 3.1 cm. As expected, the wind increased the water-level setup over the reef top. The setup at the mid-reef Gauge 8 increased quadraticly with wind speed (similar to the wind-only tests), whereas the setup at beach toe Gauge 9 followed a practically linear trend. To further understand this phenomenon, the equivalent wind-induced setup at each wind speed ($\bar{\eta}_{wind}$) was calculated from the best-fit line for the wind-only tests.
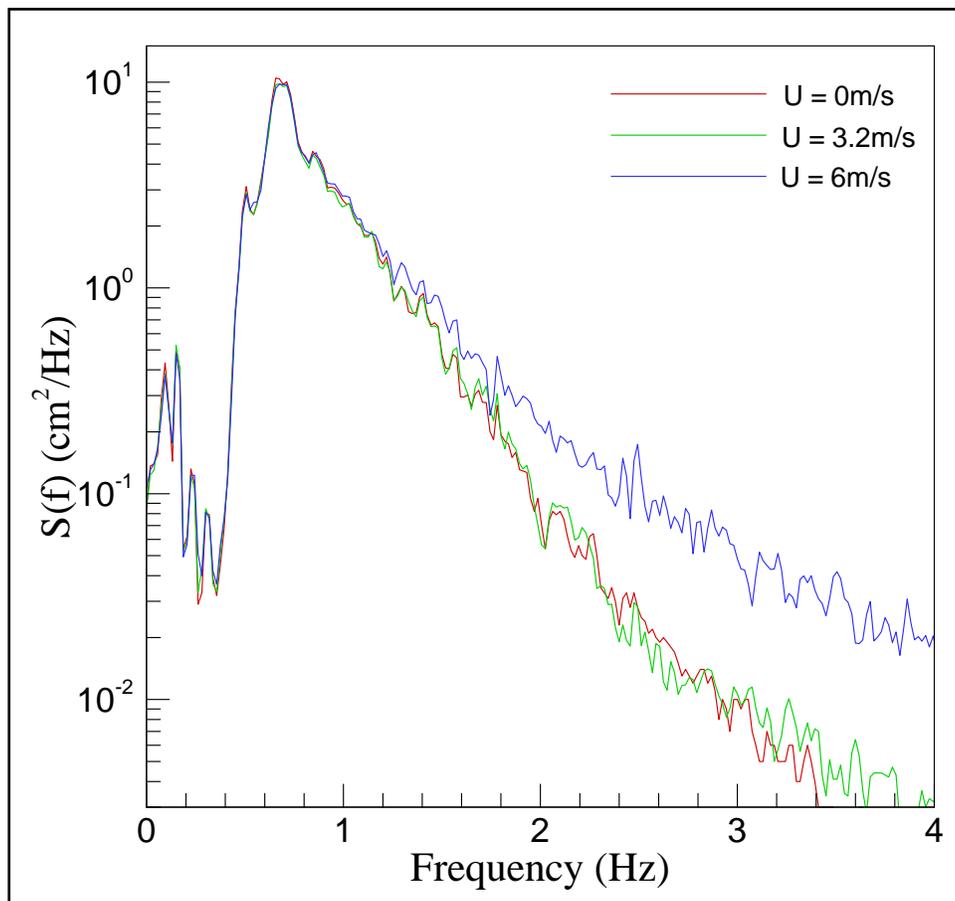
Figure 22. Wave spectral density at Gauge 2 for T_p = 1.5 sec and three wind speeds.
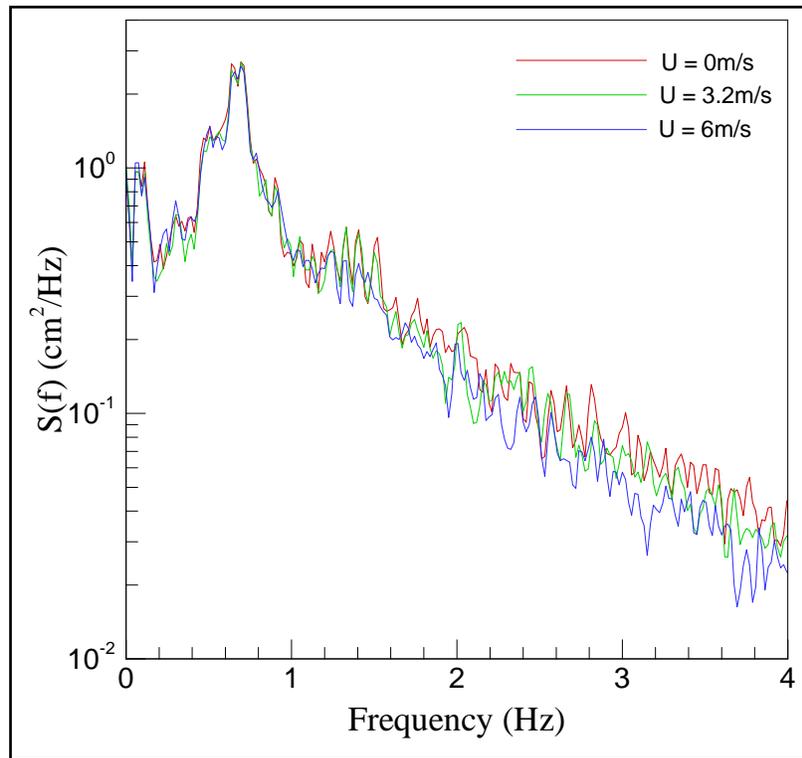
Figure 23. Wave spectral density at Gauge 7 for T_p = 1.5 sec and three wind speeds.
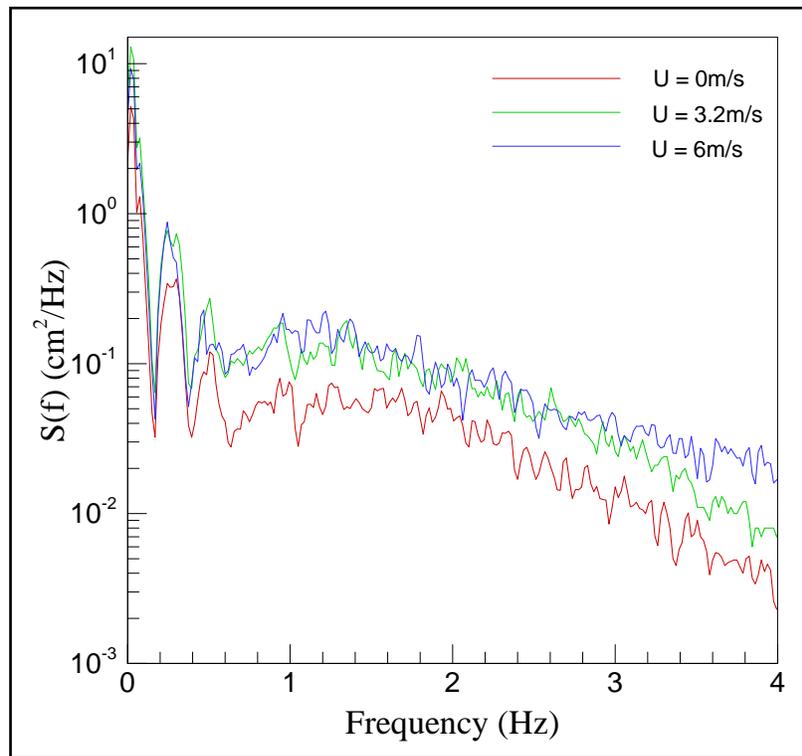
Figure 24. Wave spectral density at Gauge 9 for T_p = 1.5 sec and three wind speeds.
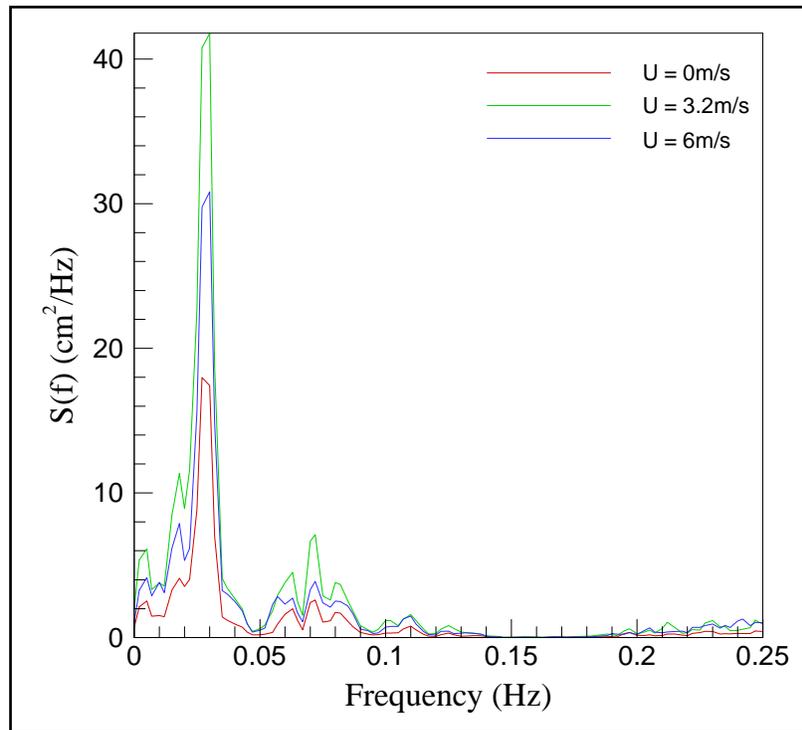
Figure 25. Low-frequency wave spectral density at Gauge 9 for T_p = 1.5 sec and three wind speeds.
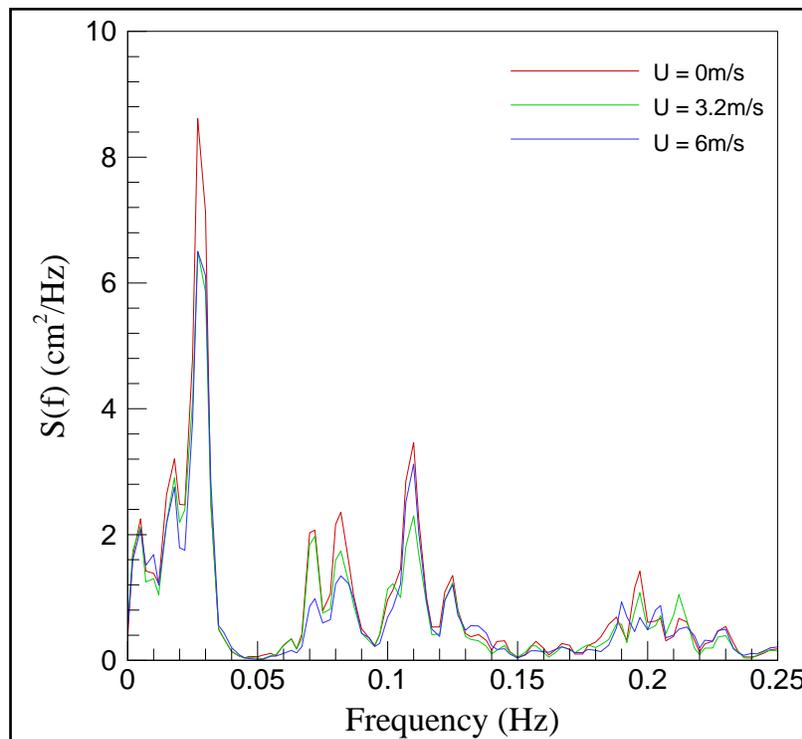
Figure 26. Low-frequency wave spectral density at Gauge 8 for T_p = 1.5 sec and three wind speeds.
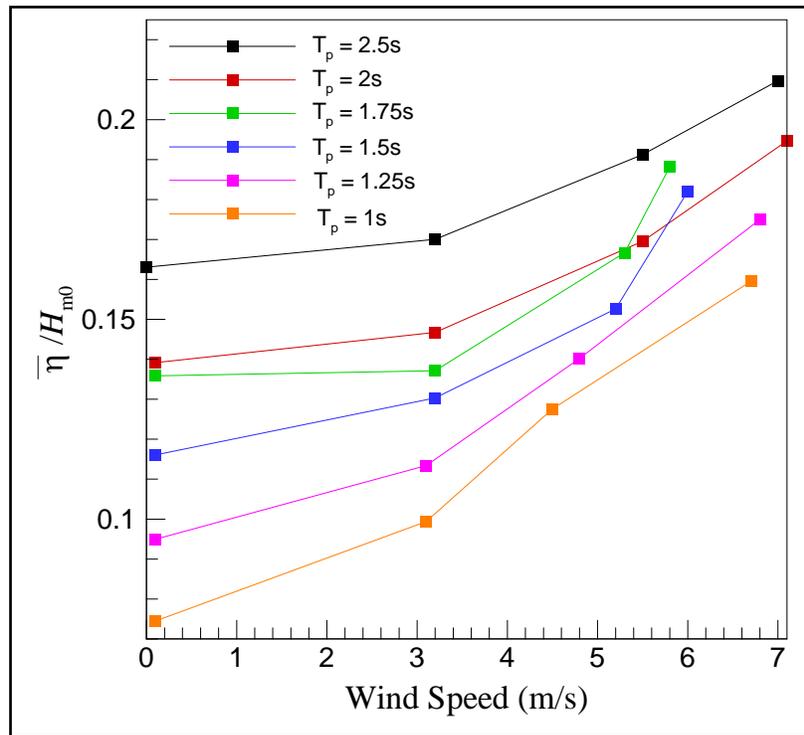
Figure 27. Relative setup versus wind speed at Gauge 8 for tests with h_r = 3.1 cm.
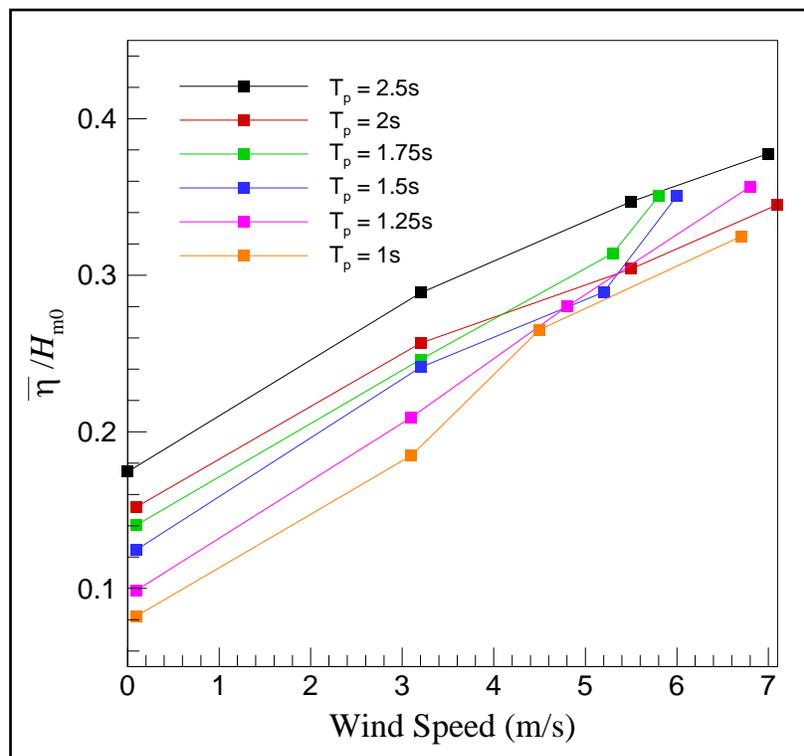
Figure 28. Relative setup versus wind speed at Gauge 9 for tests with h_r = 3.1 cm.

The difference between the setup under combined wind-wave conditions ($\bar{\eta}$), and wind only setup ($\bar{\eta}_{wind}$) are plotted in Figures 29 and 30 for Gauges 8 and 9, respectively. Figure 30 shows that the setup over the reef is enhanced under combined wind-wave conditions as compared to a linear superposition of wind-only and wave-only setups. The enhancement is weaker at mid-reef Gauge 8. One possible explanation for the higher setup value is that the increased roughness of the sea surface due to the presence of waves increases the wind-stress coefficient relative to calm water conditions (Jeffreys 1924; Miles 1957; Banner 1990; Gourlay 1996; Young 1999; Massel and Gourlay 2000; Donelan et al. 2006).
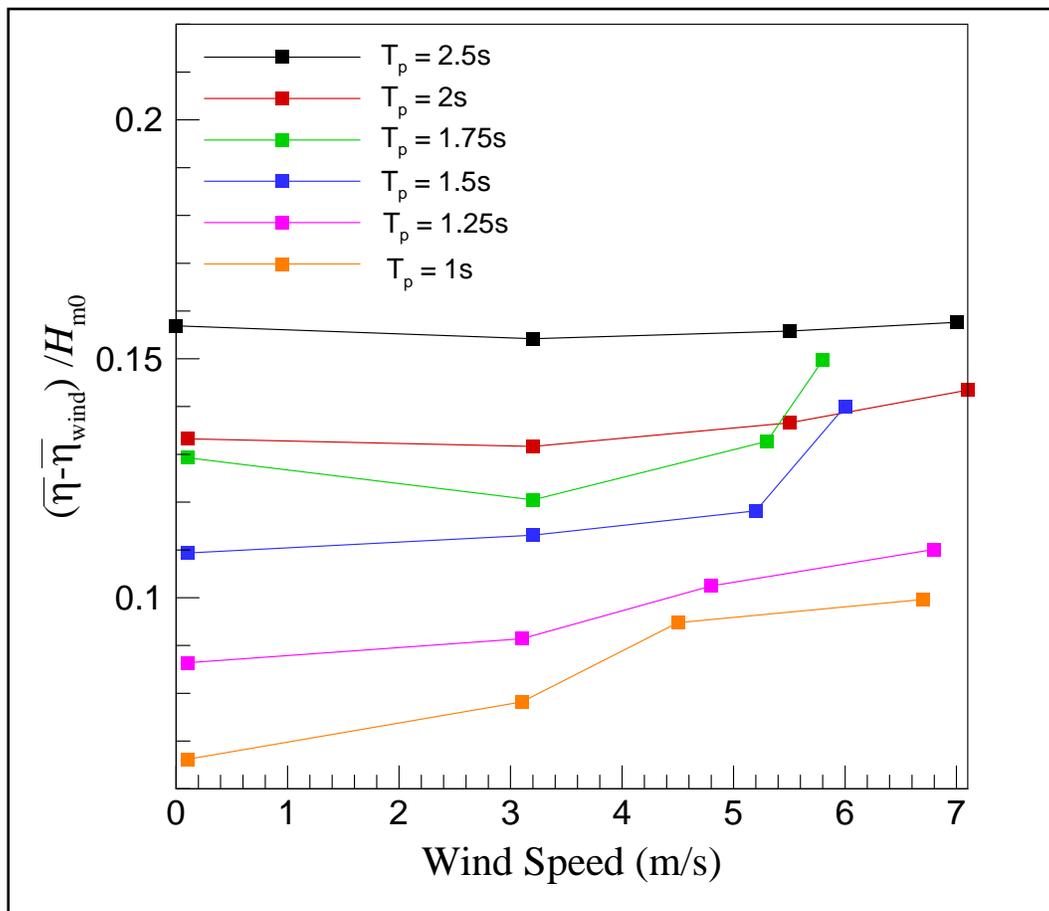
Figure 29. Relative wind-wave and wind setup difference versus wind speed at Gauge 8 for tests with h_r = 3.1 cm.
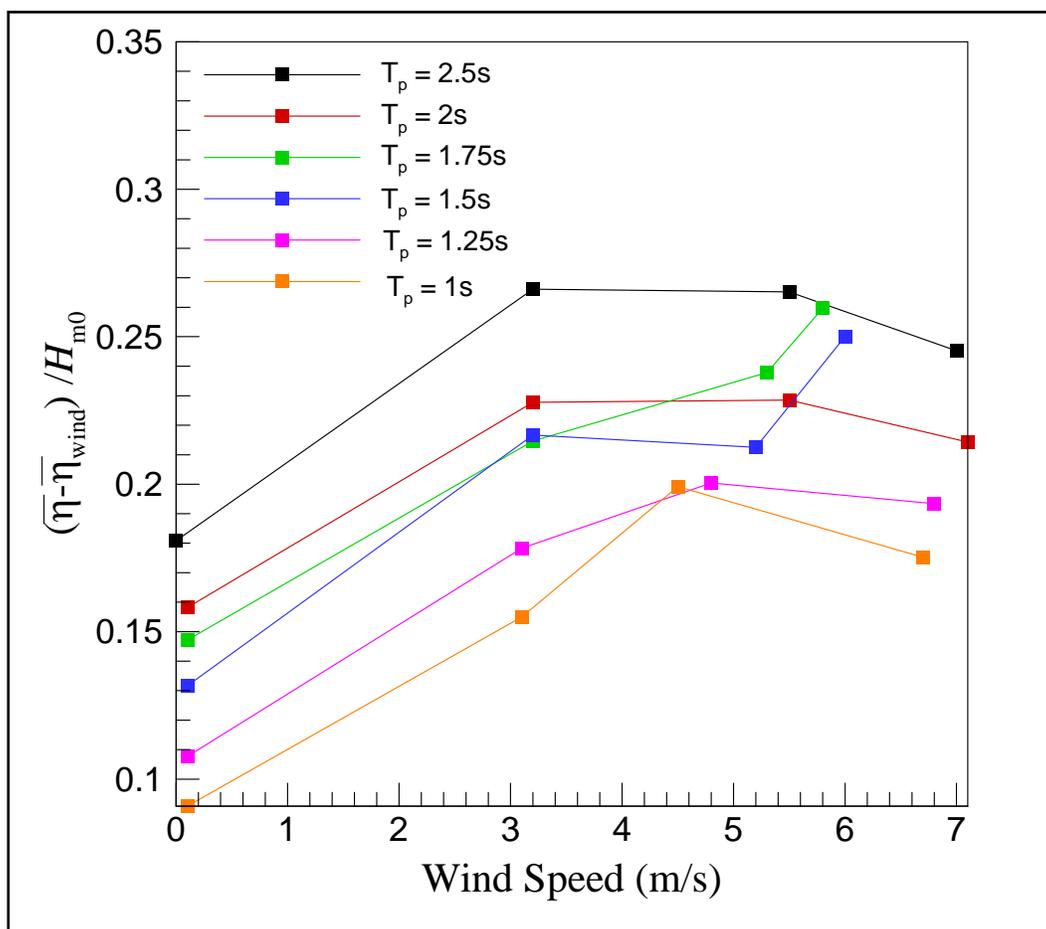
Figure 30. Relative wind-wave and wind setup difference versus wind speed at Gauge 9 for tests with h_r = 3.1 cm.

The maximum runup under combined wind-wave conditions is plotted in Figure 31 as a function of wind speed. Apart from tests at the shortest wave period T_p = 1 sec, the wind did not significantly affect the maximum runup height on the beach. The variability of the runup level exceeded by 2 percent of the runup peaks was plotted in Figure 32. Contrary to the maximum runup, a more consistent trend of increasing runup heights with increasing wind speed is observed for the $R_{2\%}$ parameter. Although the increase is somewhat weaker for low period tests (T_p = 1, 1.25 and 1.5 sec), but it is apparent.
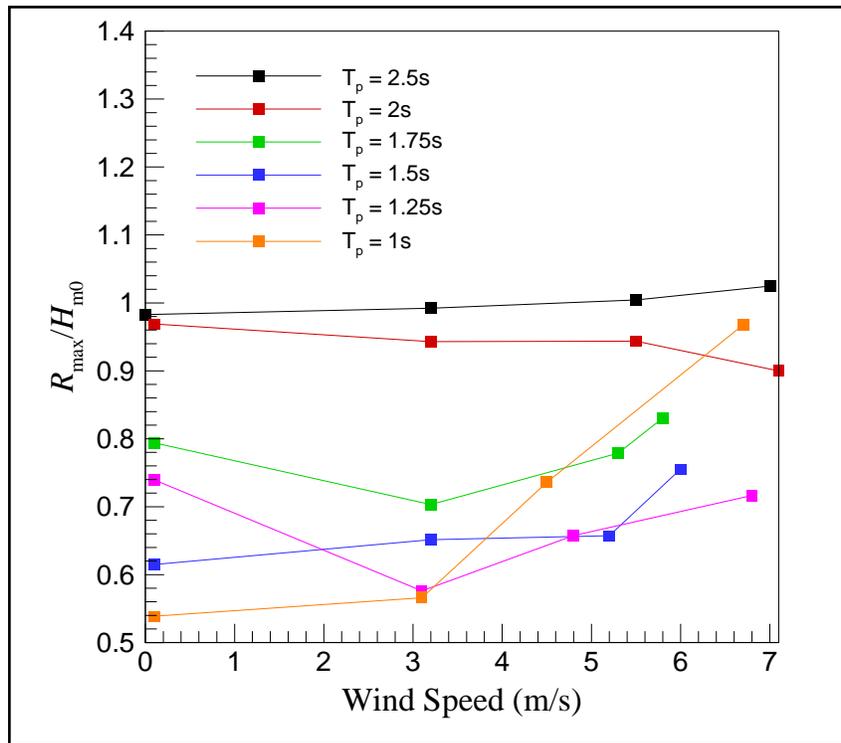
Figure 31. Relative R_{max} versus wind speed at Gauge 9 for tests with h_r = 3.1 cm.
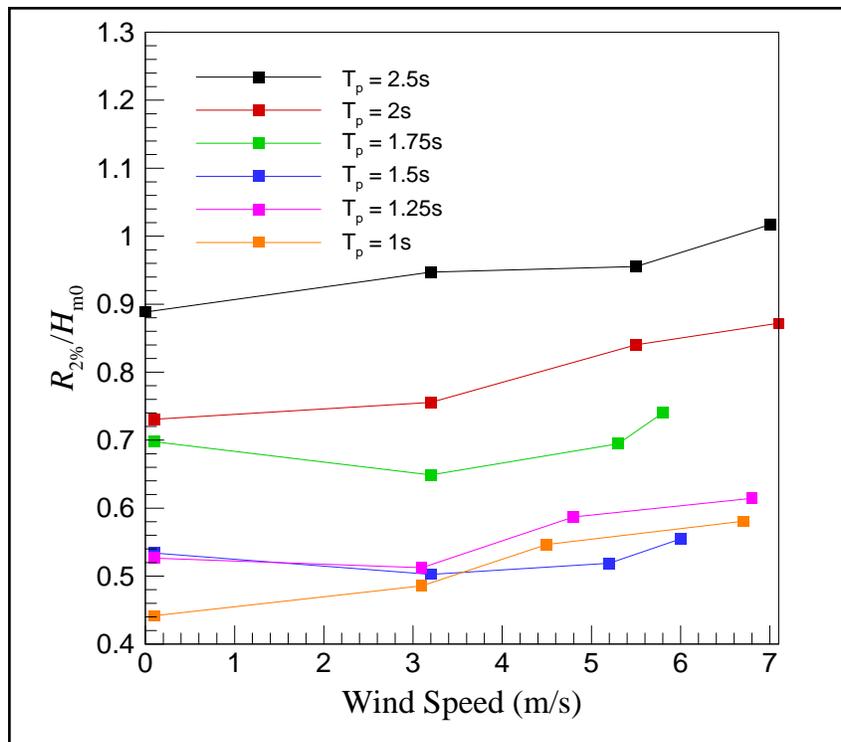
Figure 32. R2% versus wind speed at Gauge 9 for tests with h_r = 3.1 cm.

The effect of wind on the runup process can be roughly divided into static and dynamic effects: (a) static changes due to the wind-induced setup, and (b) changes due to the low-frequency oscillations over the reef. These two parts of runup are illustrated first by the difference between the $R_{2\%}$ for combined wind-wave tests and the wind-induced setup $\bar{\eta}_{wind}$, which is plotted as a function of wind speed in Figure 33. The second part of runup representing the low-frequency runup is depicted by spectral densities in Figure 34 for different wind speeds.

From Figures 33 and 34, note that the increase of runup height appears to be primarily due to wind-induced setup at the shoreline. Also note that the effect of wind on the low-frequency oscillations is complicated, deserving further research. Test results suggested that the wind enhanced the trapped oscillations at the beach toe (Figure 25), but diminished the trapped oscillations at both the mid-reef gauge (Figure 26) and runup gauge (Figure 34).
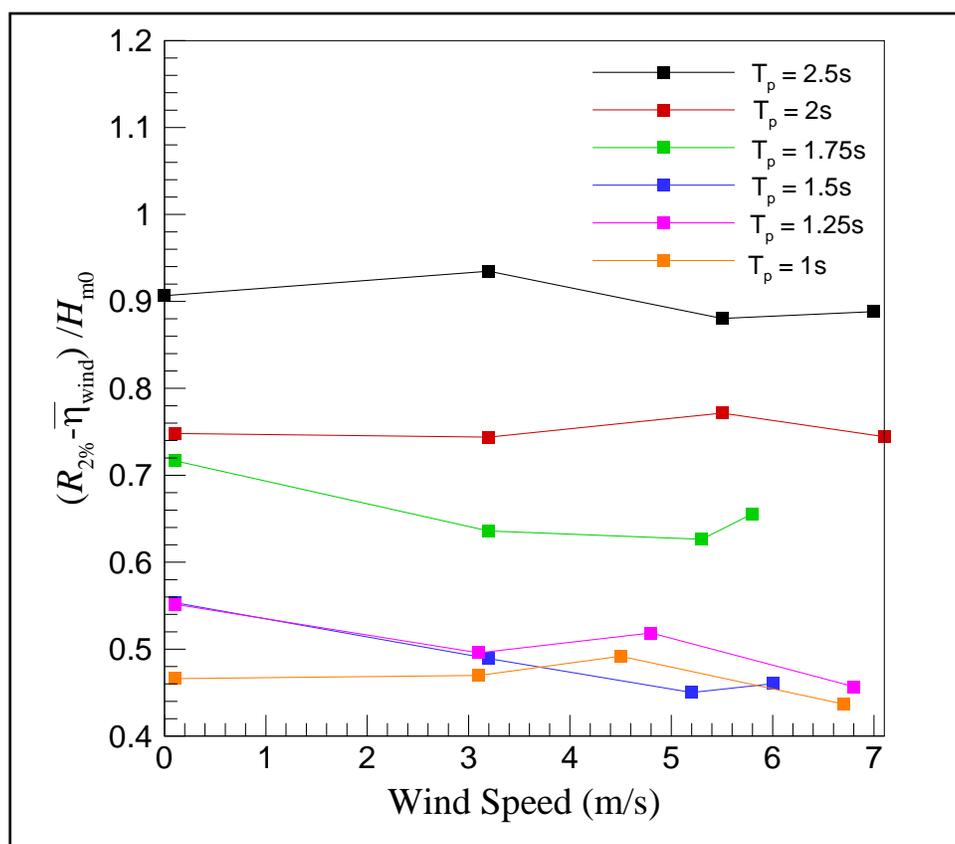
Figure 33. Difference between $R_{2\%}$ and wind setup versus wind speed at Gauge 9 for tests with h_r = 3.1 cm.
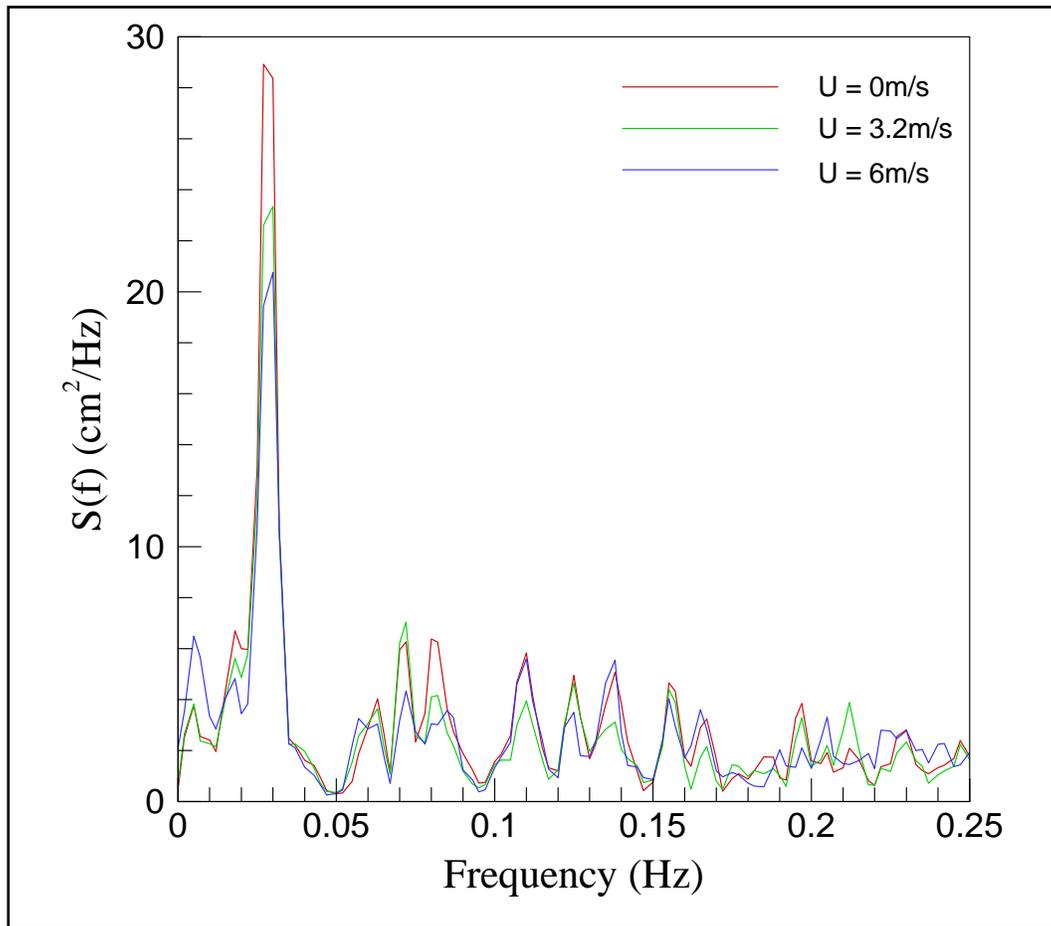
Figure 34. Low-frequency wave spectral density at Gauge 9 for tests with h_r = 3.1 cm, T_p =1.5 sec, and three wind speeds.

4   Conclusions and Recommendations

An extensive data set has been developed from this laboratory study of wind on coastal flooding over reef-type topographies. Raw data for approximately 80 test conditions are posted on the CIRP Web site. Preliminary analyses were applied to raw data, and results are included in the appendix of this report. Overall, for the range of test conditions and the reef profile investigated in this laboratory study, results showed little contribution of the wind on the measured wave maximum runup apart from static changes due to the wind-induced setup.

Results of analyses for test conditions with h_r = 3.1 cm showed that the wind increased the water-level setup over the reef top. The increase in the wave setup over the reef-top was quadratic with wind speed, whereas the setup at the beach toe gauge followed a practically linear trend. By calculating the equivalent wind-induced setup at each wind speed, $\bar{\eta}_{wind}$, from the best-fit line for the wind-only tests, the authors were able to quantify the difference between the setup under combined wind-wave conditions, $\bar{\eta}$, and wind only setup, $\bar{\eta}_{wind}$. Examination of this difference revealed that the setup over the reef is enhanced under combined wind-wave conditions as compared to a linear superposition of wind-only and wave-only setups. This greater setup value could be due to increased roughness of the sea surface caused by waves (i.e., increasing the wind-stress coefficient relative to calm water conditions).

Preliminary analysis of the maximum runup as a function of wind speed indicated that, under combined wind and waves, the wind had little or no effect on the maximum runup height on the beach except for tests with the shortest wave period, T_p = 1 sec. Another interesting finding was that in contrast to the maximum runup, R_{max}, the runup level exceeded by 2 percent of the runup peaks, $R_{2\%}$ had a more consistent trend of increasing runup heights with increasing wind speed. On this basis, $R_{2\%}$ is a more suitable parameter for engineering applications concerned about wind effects on wave runup and setup. Additional analysis of all test conditions would be necessary to determine sensitivity of runup to wind and wave parameters. As for the suitability of $R_{2\%}$ in engineering studies, this would require a comprehensive evaluation of the present data and

other data sets, and determining if the usage of $R_{2\%}$ would be commensurate with the existing practice procedures and manuals.

The preliminary analysis also indicated that the effect of wind on the runup process may be treated by a static change due to the wind-induced setup and a dynamic effect due to the low-frequency oscillations over the reef. Further investigation revealed that the increase of the runup height was primarily due to wind-induced setup at the shoreline, and the wind enhanced the trapped oscillations at the beach toe and diminished the oscillations at the top of reef. Overall, the effect of wind on the low-frequency oscillations was complicated by different type of bores developing at different water levels, requiring additional future research.

The laboratory data provided in this report may be used in studies and sensitivity testing and validation of a variety of numerical wave and circulation models. The data would help modelers to determine suitability of their models for reef applications and for calibrating runup and setup estimates for flood inundation projects. In another report, the authors will provide results of numerical modeling for the Guam reef system using the Boussinesq model BOUSS-1D/2D (Nwogu and Demirbilek 2001). The authors will parameterize the wind effect as a surface shear stress (Demirbilek et al. 1993) in the Boussinesq wave model and use the measured wave surface elevation and runup data of this experiment to evaluate the model's abilities for wave evolution over complex reef systems in the presence of winds.

The laboratory data set provided in this report is unique as test conditions represented a large parameter range for waves, winds, and water levels. Therefore, the data obtained from laboratory experiment and analyzed results should be useful in the calibration of different classes of numerical wave models for wave breaking and dissipation for waves propagating over fringing reef systems. The data provided in this report may also be used in the calibration of circulation models, including the bottom friction and eddy diffusivity coefficient.

Acknowledgments: These tests would not have been possible without the effort of technical staff of the Marine Hydrodynamics Laboratories at the University of Michigan. Special thanks to Hans Van Sumeren, the Assistant Director of the Laboratory and Nicholas Groeneweg, Erik Wilutis, and Sins Aragh for their assistance with the building and running

of the experiments. We also would like to extend our appreciation to Drs. Nicholas C. Kraus and Jane M. Smith for their reviews and comments on a draft version of this report.

References

Banner, M. L. 1990. The influence of wave breaking on the surface pressure distribution in wind-wave interaction. *Journal of Fluid Mechanics* 211: 463-495.

Demirbilek, Z., S. M. Bratos, and E. F. Thompson. 1993. *Wind products for use in coastal wave and surge models*. Miscellaneous Report CERC-93-7. Vicksburg, MS: U.S. Army Engineer Waterways Experiment Station, Coastal Engineering Research Center.

Donelan, M. A., A. Babanin, I. R. Young, and M. L. Banner. 2006. Wave-follower field measurements of the wind-input spectral function, Part II: Parameterization of the wind input. *Journal of Physical Oceanography* 6: 1,672-1,689.

Gourlay, M. R. 1996. Wave set-up on coral reefs. 1. Set-up and wave-generated flow on an idealised two dimensional horizontal reef. *Coastal Engineering* 27: 161-193.

Jeffreys, H. 1924. On the formation of waves by wind. *Proceedings of Royal Soc*iety 107A: 189-206.

Longuet-Higgins, M. S., and R. W. Stewart. 1964. Radiation stresses in water waves: A physical discussion with applications. *Deep Sea Research* 11: 529-562.

Mansard, E. P. D., and E. R. Funke. 1980. The measurement of incident and reflected spectra using a least squares method. Sydney, Australia: *International Conference on Coastal Engineering* (ICCE '80). 154–172.

Massel, S. R., and M. R. Gourlay. 2000. On the modeling of wave breaking and set-up on coral reefs. *Coastal Engineering* 39: 1-27.

Miles, J. W. 1957. On the generation of surface waves by shear flows. *Journal of Fluid Mechanics* 3: 185-204.

Nwogu, O., and Z. Demirbilek. 2001. *BOUSS-2D: A Boussinesq wave model for coastal regions and harbors*. ERDC/CHL TR-01-25. Vicksburg, MS: U.S. Army Engineer Research and Development Center, Coastal and Hydraulics Laboratory.

Seelig, W. N. 1983. Laboratory study of reef-lagoon system hydraulics. *Journal of Waterway, Port, Coastal, and Ocean Engineering,* American Society of Civil Engineers. 109: 380-391.

Symonds, G., D. A. Huntley, and A. J. Bowen. 1982. Two-dimensional surf beat: Long wave generation by a time-varying breakpoint. *Journal of Geophysical Research* 87: 492-498.

Wu, J. 1969. Froude number scaling of wind-stress coefficients. *Journal of the Atmospheric Sciences* 26: 408-413.

Young, I. R. 1999. *Wind generated ocean waves*. New York: Elsevier.

Appendix: Analyzed Data

Table A1. Test 15 (H = 6.2 cm, T = 1.0 sec, WL = 55.1 cm).

Gauge No.	H_{m0} (cm)	T_p (sec)	$\bar{\eta}$ (cm)
1	6.6	1.0	-0.2
2	6.2	1.0	0.0
3	6.2	1.0	0.0
4	3.9	1.0	0.0
5	5.7	1.0	-0.1
6	5.9	1.1	-0.1
7	-	-	-
8	2.7	8.8	0.4
9	2.5	38.1	0.5
R_{max} = 3.3 cm, $R_{2\%}$ = 2.7 cm, $R_{10\%}$ = 2.5 cm, V_{wind} = 0. 1 m/sec			

Table A2. Test 16 (H = 5.2 cm, T = 1.5 sec, WL = 55.1 cm).

Gauge No.	H_{m0} (cm)	T_p (sec)	$\bar{\eta}$ (cm)
1	5.5	1.5	-0.1
2	5.2	1.5	0.0
3	5.3	1.5	0.0
4	3.6	1.5	0.0
5	5.2	1.5	-0.1
6	5.7	1.5	-0.1
7	4.9	1.5	0.1
8	2.6	38.1	0.4
9	2.6	38.1	0.5
R_{max} = 3.2 cm, $R_{2\%}$ = 2.6 cm, $R_{10\%}$ = 2.4 cm, V_{wind} = 0. 1 m/sec			

Table A3. Test 17 (H = 7.8 cm, T = 1.5 sec, WL = 55.1 cm).

Gauge No.	H_{m0} (cm)	T_p (sec)	$\bar{\eta}$ (cm)
1	8.3	1.5	-0.2
2	7.8	1.5	-0.1
3	7.9	1.5	-0.1
4	5.3	1.5	-0.1
5	7.9	1.5	-0.2
6	8.3	1.5	-0.2
7	6.0	1.5	0.3
8	3.3	38.1	0.7
9	3.3	38.1	0.8
R_{max} = 5.5 cm, $R_{2\%}$ = 3.8 cm, $R_{10\%}$ = 3.4 cm, V_{wind} = 0.1 m/sec			

Table A4. Test 18 (H = 8.5 cm, T = 2.0 sec, WL = 55.1 cm).

Gauge No.	H_{m0} (cm)	T_p (sec)	$\bar{\eta}$ (cm)
1	9.2	2.0	-0.2
2	8.5	2.0	-0.1
3	8.4	2.0	-0.1
4	6.4	2.1	-0.2
5	9.5	2.1	-0.2
6	9.4	2.1	-0.3
7	7.0	2.2	0.4
8	4.4	38.1	1.0
9	4.6	38.1	1.1
R_{max} = 8.4 cm, $R_{2\%}$ = 6.4 cm, $R_{10\%}$ = 5.2 cm, V_{wind} = 0.1 m/sec			

Table A5. Test 19 (H = 8.3 cm, T = 2.5 sec, WL = 55.1 cm).

Gauge No.	H_{m0} (cm)	T_p (sec)	$\bar{\eta}$ (cm)
1	8.9	2.5	-0.3
2	8.3	2.5	-0.2
3	8.2	2.5	-0.2
4	6.6	2.5	-0.2
5	10.3	2.6	-0.3
6	10.0	2.5	-0.4
7	7.4	2.6	0.5
8	4.7	38.1	1.1
9	5.1	38.1	1.2
R_{max} = 8.9 cm, $R_{2\%}$ = 6.1 cm, $R_{10\%}$ = 5.7 cm, V_{wind} = 0.1 m/sec			

Table A6. Test 20 (H = 6.1 cm, T = 1.25 sec, WL = 55.1 cm).

Gauge No.	H_{m0} (cm)	T_p (sec)	$\bar{\eta}$ (cm)
1	6.5	1.2	-0.2
2	6.1	1.2	-0.1
3	6.1	1.3	0.0
4	4.0	1.2	0.0
5	5.8	1.3	-0.1
6	6.3	1.3	-0.1
7	5.1	1.3	0.2
8	2.7	38.1	0.5
9	2.6	38.1	0.5
R_{max} = 3.2 cm, $R_{2\%}$ = 2.7 cm, $R_{10\%}$ = 2.6 cm, V_{wind} = 0.1 m/sec			

Table A7. Test 21 (H = 8.2 cm, T = 1.75 sec, WL = 55.1 cm).

Gauge No.	H_{m0} (cm)	T_p (sec)	$\bar{\eta}$ (cm)
1	8.8	1.8	-0.2
2	8.2	1.8	-0.1
3	8.1	1.8	-0.1
4	5.8	1.8	-0.1
5	8.7	1.8	-0.2
6	8.9	1.8	-0.3
7	6.6	1.8	0.4
8	3.9	38.1	0.8
9	4.0	38.1	0.9
R_{max} = 7.2 cm, $R_{2\%}$ = 5.1 cm, $R_{10\%}$ = 4.4 cm, V_{wind} = 0.1 m/sec			

Table A8. Test 26 (H = 5.8 cm, T = 1.0 sec, WL = 51.6 cm).

Gauge No.	H_{m0} (cm)	T_p (sec)	$\bar{\eta}$ (cm)
1	6.2	1.0	-0.2
2	5.8	1.0	-0.1
3	5.9	1.0	-0.1
4	4.0	1.0	-0.1
5	5.4	1.0	-0.1
6	5.3	1.0	-0.2
7	2.7	1.1	0.7
8	1.4	57.1	0.9
9	1.5	38.1	0.8
R_{max} = 2.2 cm, $R_{2\%}$ = 2.0 cm, $R_{10\%}$ =1.8 cm, V_{wind} = 0.1 m/sec			

Table A9. Test 27 (H = 5.5 cm, T = 1.25 sec, WL = 51.6 cm).

Gauge No.	H_{m0} (cm)	T_p (sec)	$\bar{\eta}$ (cm)
1	5.9	1.2	-0.2
2	5.5	1.2	-0.1
3	5.5	1.2	-0.1
4	3.9	1.2	-0.1
5	5.4	1.2	-0.2
6	5.7	1.3	-0.2
7	3.0	1.3	0.7
8	1.6	57.1	0.9
9	1.7	57.1	1.0
R_{max} = 2.5 cm, $R_{2\%}$ = 2.3 cm, $R_{10\%}$ =1.9 cm, V_{wind} = 0.1 m/sec			

Table A10. Test 28 (H = 4.7 cm, T = 1.5 sec, WL = 51.6 cm).

Gauge No.	H_{m0} (cm)	T_p (sec)	$\bar{\eta}$ (cm)
1	5.0	1.5	-0.2
2	4.7	1.5	-0.1
3	4.7	1.5	-0.1
4	3.5	1.4	-0.1
5	4.9	1.5	-0.2
6	5.4	1.4	-0.2
7	3.0	2.0	0.6
8	1.5	57.1	0.9
9	1.5	57.1	1.0
R_{max} = 3.0 cm, $R_{2\%}$ = 2.0 cm, $R_{10\%}$ =1.8 cm, V_{wind} = 0.1 m/sec			

Table A11. Test 29 (H = 7.1 cm, T = 1.5 sec, WL = 51.6 cm).

Gauge No.	H_{m0} (cm)	T_p (sec)	$\bar{\eta}$ (cm)
1	7.5	1.5	-0.3
2	7.1	1.5	-0.2
3	7.1	1.5	-0.2
4	5.2	1.5	-0.2
5	7.3	1.5	-0.3
6	7.2	1.4	-0.3
7	3.7	1.9	1.0
8	2.1	57.1	1.3
9	2.1	38.1	1.4
R_{max} = 4.0 cm, $R_{2\%}$ = 3.2 cm, $R_{10\%}$ =2.9 cm, V_{wind} = 0.1 m/sec			

Table A12. Test 30 (H = 7.6 cm, T = 1.75 sec, WL = 51.6 cm).

Gauge No.	H_{m0} (cm)	T_p (sec)	$\bar{\eta}$ (cm)
1	8.2	1.8	-0.3
2	7.6	1.8	-0.2
3	7.5	1.9	-0.2
4	5.9	1.9	-0.3
5	8.2	1.9	-0.3
6	7.3	1.8	-0.3
7	4.1	1.8	1.1
8	2.4	57.1	1.4
9	2.6	38.1	1.6
R_{max} = 5.6 cm, $R_{2\%}$ = 4.0 cm, $R_{10\%}$ =3.8 cm, V_{wind} = 0.1 m/sec			

Table A13. Test 31 (*H* = 8.5 cm, *T* = 2.0 sec, *WL* = 51.6 cm).

Gauge No.	H_{m0} (cm)	T_p (sec)	$\bar{\eta}$ (cm)
1	9.2	2.0	-0.4
2	8.5	2.0	-0.3
3	8.2	2.0	-0.2
4	6.8	2.0	-0.3
5	9.3	2.2	-0.4
6	7.7	2.2	-0.3
7	4.5	2.2	1.2
8	2.9	38.1	1.7
9	3.3	38.1	1.9
R_{max} = 9.0 cm, $R_{2\%}$ = 5.0 cm, $R_{10\%}$ =4.7 cm, V_{wind} = 0.1 m/sec			

Table A14. Test 32 (*H* = 7.9 cm, *T* = 2.5 sec, *WL* = 51.6 cm).

Gauge No.	H_{m0} (cm)	T_p (sec)	$\bar{\eta}$ (cm)
1	8.5	2.5	-0.4
2	7.9	2.5	-0.3
3	7.9	2.5	-0.3
4	6.8	2.4	-0.4
5	9.9	2.4	-0.4
6	8.1	2.6	-0.4
7	5.0	2.6	1.3
8	3.2	38.1	1.8
9	3.6	38.1	2.0
R_{max} = 8.7 cm, $R_{2\%}$ = 5.4 cm, $R_{10\%}$ =5.2 cm, V_{wind} = 0.1 m/sec			

Table A15. Test 33 (*H* = 5.6 cm, *T* = 1.0 sec, *WL* = 50.0 cm).

Gauge No.	H_{m0} (cm)	T_p (sec)	$\bar{\eta}$ (cm)
1	6.0	1.0	-0.2
2	5.6	1.0	-0.1
3	5.7	1.0	-0.1
4	4.0	1.0	-0.1
5	5.3	1.0	-0.2
6	4.9	1.0	-0.2
7	1.7	28.6	0.6
8	1.0	114.3	0.9
9	1.0	114.3	1.1
R_{max} = 0.4 cm, $R_{2\%}$ = 0.0 cm, $R_{10\%}$ =0.0 cm, V_{wind} = 0.1 m/sec			

Table A16. Test 34 (H = 4.5 cm, T = 1.5 sec, WL = 50.0 cm).

Gauge No.	H_{m0} (cm)	T_p (sec)	$\bar{\eta}$ (cm)
1	4.8	1.5	-0.2
2	4.5	1.5	-0.2
3	4.5	1.5	-0.2
4	3.5	1.5	-0.2
5	4.8	1.5	-0.2
6	5.1	1.4	-0.3
7	2.0	114.3	0.8
8	1.1	114.3	1.2
9	1.2	114.3	1.2
R_{max} = 0.9 cm, $R_{2\%}$ = 0.1 cm, $R_{10\%}$ =0.1 cm, V_{wind} = 0.0 m/sec			

Table A17. Test 35 (H = 4.5 cm, T = 1.5 sec, WL = 50.0 cm).

Gauge No.	H_{m0} (cm)	T_p (sec)	$\bar{\eta}$ (cm)
1	4.8	1.5	-0.2
2	4.5	1.5	-0.2
3	4.5	1.5	-0.2
4	3.5	1.5	-0.2
5	4.8	1.5	-0.2
6	5.1	1.4	-0.3
7	2.0	114.3	0.8
8	1.1	114.3	1.1
9	1.2	114.3	1.3
R_{max} =1.0 cm, $R_{2\%}$ = 0.1 cm, $R_{10\%}$ =0.1 cm, V_{wind} = 0.0 m/sec			

Table A18. Test 36 (H = 6.8 cm, T = 1.5 sec, WL = 50.0 cm).

Gauge No.	H_{m0} (cm)	T_p (sec)	$\bar{\eta}$ (cm)
1	7.3	1.5	-0.3
2	6.8	1.5	-0.3
3	6.8	1.5	-0.2
4	5.2	1.5	-0.3
5	7.0	1.5	-0.3
6	6.5	1.5	-0.3
7	2.7	114.3	1.2
8	1.5	114.3	1.6
9	1.6	114.3	1.8
R_{max} = 2.0 cm, $R_{2\%}$ = 1.4 cm, $R_{10\%}$ =1.3 cm, V_{wind} = 0.0 m/sec			

Table A19. Test 37 (*H* = 7.6 cm, *T* = 1.75 sec, *WL* = 50.0 cm).

Gauge No.	H_{m0} (cm)	T_p (sec)	$\bar{\eta}$ (cm)
1	8.2	1.8	-0.4
2	7.6	1.8	-0.3
3	7.4	1.8	-0.3
4	6.1	1.8	-0.3
5	7.9	1.8	-0.4
6	6.7	1.8	-0.3
7	3.1	2.0	1.3
8	1.8	57.1	1.7
9	2.1	38.1	2.0
R_{max} = 4.1 cm, $R_{2\%}$ = 2.8 cm, $R_{10\%}$ =2.4 cm, V_{wind} = 0.1 m/sec			

Table A20. Test 38 (*H* = 8.4 cm, *T* = 2.0 sec, *WL* = 50.0 cm).

Gauge No.	H_{m0} (cm)	T_p (sec)	$\bar{\eta}$ (cm)
1	9.1	2.0	-0.4
2	8.4	2.0	-0.3
3	8.2	2.0	-0.3
4	7.0	2.0	-0.4
5	8.9	2.2	-0.4
6	6.9	2.2	-0.2
7	3.4	2.2	1.5
8	2.1	57.1	1.9
9	2.6	38.1	2.2
R_{max} = 5.5 cm, $R_{2\%}$ = 3.8 cm, $R_{10\%}$ =3.4 cm, V_{wind} = 0.0 m/sec			

Table A21. Test 39 (*H* = 7.7 cm, *T* = 2.5 sec, *WL* = 50.0 cm).

Gauge No.	H_{m0} (cm)	T_p (sec)	$\bar{\eta}$ (cm)
1	8.3	2.5	-0.5
2	7.7	2.5	-0.4
3	7.6	2.5	-0.3
4	6.9	2.4	-0.4
5	9.4	2.4	-0.5
6	7.2	2.5	-0.3
7	3.8	2.5	1.6
8	2.4	57.1	2.1
9	2.8	38.1	2.4
R_{max} = 4.8 cm, $R_{2\%}$ = 4.1 cm, $R_{10\%}$ =3.5 cm, V_{wind} = 0.0 m/sec			

Table A22. Test 44 (H = 3.2 cm, T = 1.0 sec, WL = 53.1 cm).

Gauge No.	H_{m0} (cm)	T_p (sec)	$\bar{\eta}$ (cm)
1	3.4	1.0	-0.4
2	3.2	1.0	0.0
3	3.2	1.0	0.1
4	2.1	1.0	0.0
5	2.9	1.0	0.0
6	3.1	1.0	-0.1
7	3.0	1.0	0.1
8	1.6	57.1	0.3
9	1.2	38.1	0.2
R_{max} = 2.3 cm, $R_{2\%}$ = 1.6 cm, $R_{10\%}$ =1.4 cm, V_{wind} = 0.0 m/s			

Table A23. Test 45 (H = 6.1 cm, T = 1.0 sec, WL = 53.1 cm).

Gauge No.	H_{m0} (cm)	T_p (sec)	$\bar{\eta}$ (cm)
1	6.3	1.0	-0.3
2	6.1	1.0	-0.1
3	6.1	1.0	0.0
4	4.0	1.0	-0.1
5	5.5	1.0	-0.1
6	5.7	1.1	-0.1
7	4.1	1.1	0.2
8	2.1	9.5	0.5
9	1.7	38.1	0.5
R_{max} = 3.3 cm, $R_{2\%}$ = 2.6 cm, $R_{10\%}$ =2.4 cm, V_{wind} = 0.1 m/sec			

Table A24. Test 46 (H = 5.9 cm, T = 1.25 sec, WL = 53.1 cm).

Gauge No.	H_{m0} (cm)	T_p (sec)	$\bar{\eta}$ (cm)
1	6.2	1.2	-0.4
2	5.9	1.2	-0.1
3	5.8	1.3	-0.1
4	4.0	1.2	-0.1
5	5.7	1.3	-0.2
6	6.1	1.3	-0.2
7	4.3	1.2	0.4
8	2.2	38.1	0.6
9	2.1	38.1	0.6
R_{max} = 4.3 cm, $R_{2\%}$ = 3.1 cm, $R_{10\%}$ =2.9 cm, V_{wind} = 0.1 m/sec			

Table A25. Test 47 (*H* = 5.0 cm, *T* = 1.5 sec, *WL* = 53.1 cm).

Gauge No.	H_{m0} (cm)	T_p (sec)	$\bar{\eta}$ (cm)
1	5.2	1.5	-0.3
2	5.0	1.5	-0.1
3	5.0	1.5	-0.1
4	3.5	1.5	-0.1
5	5.1	1.5	-0.1
6	5.6	1.5	-0.2
7	4.4	1.5	0.3
8	2.1	38.1	0.5
9	1.9	38.1	0.6
R_{max} = 3.7 cm, R$_{2\%}$ = 3.0 cm, R$_{10\%}$ =2.7 cm, V_{wind} = 0.1 m/sec			

Table A26. Test 48 (*H* = 7.5 cm, *T* = 1.5 sec, *WL* = 53.1 cm).

Gauge No.	H_{m0} (cm)	T_p (sec)	$\bar{\eta}$ (cm)
1	7.9	1.5	-0.3
2	7.5	1.5	-0.1
3	7.5	1.5	-0.2
4	5.3	1.5	-0.2
5	7.6	1.5	-0.2
6	7.9	1.5	-0.3
7	5.0	1.5	0.6
8	2.8	38.1	0.9
9	2.7	38.1	0.9
R_{max} = 4.6 cm, R$_{2\%}$ = 4.1 cm, R$_{10\%}$ =3.8 cm, V_{wind} = 0.1 m/sec			

Table A27. Test 57 (*H* = 7.7 cm, *T* = 1.75 sec, *WL* = 53.1 cm).

Gauge No.	H_{m0} (cm)	T_p (sec)	$\bar{\eta}$ (cm)
1	8.3	1.8	-0.3
2	7.7	1.8	-0.2
3	7.6	1.8	-0.2
4	5.8	1.8	-0.2
5	8.1	1.8	-0.3
6	8.2	1.8	-0.3
7	5.6	1.8	0.7
8	3.1	38.1	1.1
9	3.2	38.1	1.1
R_{max} = 7.5 cm, R$_{2\%}$ =5.5 cm, R$_{10\%}$ =4.8 cm, V_{wind} = 0.1 m/sec			

Table A28. Test 58 (*H* = 8.5 cm, *T* = 2.0 sec, *WL* = 53.1 cm).

Gauge No.	H_{m0} (cm)	T_p (sec)	$\bar{\bar{\eta}}$ (cm)
1	9.3	2.0	-0.3
2	8.6	2.0	-0.2
3	8.4	2.0	-0.2
4	6.7	2.1	-0.2
5	9.2	2.1	-0.4
6	8.7	2.1	-0.3
7	6.1	2.2	0.8
8	3.8	38.1	1.2
9	4.1	38.1	1.3
R_{max} = 8.3 cm, R$_{2\%}$ =6.3 cm, R$_{10\%}$ =5.7 cm, V_{wind} = 0.1 m/sec			

Table A29. Test 59 (*H* = 8.2 cm, *T* = 2.5 sec, *WL* = 53.1 cm).

Gauge No.	H_{m0} (cm)	T_p (sec)	$\bar{\bar{\eta}}$ (cm)
1	8.8	2.5	-0.4
2	8.2	2.5	-0.2
3	8.1	2.5	-0.2
4	6.8	2.5	-0.3
5	9.9	2.5	-0.5
6	9.2	2.6	-0.4
7	6.4	2.6	0.9
8	4.0	38.1	1.3
9	4.5	38.1	1.4
R_{max} = 8.0 cm, R$_{2\%}$ =7.3 cm, R$_{10\%}$ =6.3 cm, V_{wind} = 0.1 m/sec			

Table A30. Test 60 (*H* = 8.1 cm, *T* = 2.5 sec, *WL* = 53.1 cm).

Gauge No.	H_{m0} (cm)	T_p (sec)	$\bar{\bar{\eta}}$ (cm)
1	6.7	38.1	-0.3
2	8.1	2.5	-0.2
3	8.1	2.5	-0.4
4	6.6	2.5	-0.2
5	9.8	2.6	-0.5
6	9.1	2.6	-0.5
7	-	-	-
8	3.9	38.1	1.4
9	6.1	38.1	2.3
R_{max} = 8.1 cm, R$_{2\%}$ =7.7 cm, R$_{10\%}$ =6.3 cm, V_{wind} = 3.2 m/sec			

Table A31. Test 61 (*H* = 8.5 cm, *T* = 2.0 sec, *WL* = 53.1 cm).

Gauge No.	H_{m0} (cm)	T_p (sec)	$\bar{\eta}$ (cm)
1	9.4	2.0	-0.2
2	8.5	2.0	-0.1
3	8.3	2.0	-0.1
4	6.6	2.1	-0.2
5	9.1	2.1	-0.4
6	8.6	2.1	-0.3
7	-	-	-
8	3.6	38.1	1.1
9	5.7	38.1	2.1
R_{max} = 8.0 cm, $R_{2\%}$ =6.4 cm, $R_{10\%}$ =5.7 cm, V_{wind} = 3.2 m/sec			

Table A32. Test 62 (*H* = 7.7 cm, *T* = 1.75 sec, *WL* = 53.1 cm).

Gauge No.	H_{m0} (cm)	T_p (sec)	$\bar{\eta}$ (cm)
1	8.4	1.8	-0.1
2	7.7	1.8	-0.1
3	7.6	1.8	-0.1
4	5.7	1.8	-0.1
5	7.9	1.8	-0.4
6	8.0	1.8	-0.4
7	-	-	-
8	3.0	38.1	1.1
9	4.8	38.1	1.9
R_{max} =5.4 cm, $R_{2\%}$ =5.0 cm, $R_{10\%}$ =4.5 cm, V_{wind} = 3.2 m/sec			

Table A33. Test 63 (*H* = 7.4 cm, *T* = 1.5 sec, *WL* = 53.1 cm).

Gauge No.	H_{m0} (cm)	T_p (sec)	$\bar{\eta}$ (cm)
1	8.1	1.5	-0.2
2	7.4	1.5	-0.1
3	7.4	1.5	-0.1
4	5.2	1.5	-0.2
5	7.2	1.5	-0.3
6	7.7	1.5	-0.3
7	-	-	-
8	2.5	38.1	1.0
9	4.1	38.1	1.8
R_{max} =4.8 cm, $R_{2\%}$ =3.7 cm, $R_{10\%}$ =3.5 cm, V_{wind} = 3.2 m/sec			

Table A34. Test 64 (*H* = 4.9 cm, *T* =1 .5 sec, *WL* = 53.1 cm).

Gauge No.	H_{m0} (cm)	T_p (sec)	$\bar{\eta}$ (cm)
1	5.3	1.5	-0.1
2	4.9	1.5	-0.1
3	4.9	1.5	-0.1
4	3.5	1.5	-0.1
5	4.9	1.5	-0.2
6	5.6	1.5	-0.2
7	-	-	-
8	2.0	38.1	0.6
9	3.2	38.1	1.1
R_{max} = 3.3 cm, $R_{2\%}$ =2.9 cm, $R_{10\%}$ =2.6 cm, V_{wind} = 3.1 m/sec			

Table A35. Test 65 (*H* = 5.8 cm, *T* = 1.25 sec, *WL* = 53.1 cm).

Gauge No.	H_{m0} (cm)	T_p (sec)	$\bar{\eta}$ (cm)
1	6.3	1.2	-0.1
2	5.8	1.2	-0.1
3	5.7	1.2	-0.1
4	3.9	1.2	-0.1
5	5.4	1.2	-0.2
6	6.0	1.2	-0.2
7	4.1	1.2	0.4
8	2.1	38.1	0.7
9	3.4	38.1	1.2
R_{max} = 3.3 cm, $R_{2\%}$ =3.0 cm, $R_{10\%}$ =2.8 cm, V_{wind} = 3.1 m/sec			

Table A36. Test 66 (*H* = 6.0 cm, *T* = 1.0 sec, *WL* = 53.1 cm).

Gauge No.	H_{m0} (cm)	T_p (sec)	$\bar{\eta}$ (cm)
1	6.5	1.0	-0.1
2	6.0	1.0	-0.1
3	5.9	1.0	0.0
4	3.9	1.0	-0.1
5	5.4	1.0	-0.2
6	5.6	1.1	-0.1
7	3.8	1.1	0.3
8	2.0	9.5	0.6
9	3.0	38.1	1.1
R_{max} = 3.4 cm, $R_{2\%}$ =2.9 cm, $R_{10\%}$ =2.6 cm, V_{wind} = 3.1 m/sec			

Table A37. Test 67 (H = 3.2 cm, T = 1.0 sec, WL = 53.1 cm).

Gauge No.	H_{m0} (cm)	T_p (sec)	$\bar{\eta}$ (cm)
1	3.5	1.0	-0.1
2	3.2	1.0	0.0
3	3.2	1.0	0.0
4	2.1	1.0	0.0
5	2.9	1.0	-0.1
6	3.2	1.0	0.0
7	-	-	-
8	1.5	57.1	0.3
9	2.3	38.1	0.5
R_{max} = 2.3 cm, $R_{2\%}$ =1.6 cm, $R_{10\%}$ =1.5 cm, V_{wind} = 3.1 m/sec			

Table A38. Test 68 (H = 8.1 cm, T = 2.5 sec, WL = 53.1 cm).

Gauge No.	H_{m0} (cm)	T_p (sec)	$\bar{\eta}$ (cm)
1	9.0	2.5	-0.4
2	8.1	2.5	-0.2
3	8.0	2.5	-0.3
4	6.7	2.5	-0.3
5	9.7	2.6	-0.5
6	9.0	2.6	-0.4
7	-	-	-
8	3.8	38.1	1.6
9	6.0	38.1	2.8
R_{max} = 8.1 cm, $R_{2\%}$ =7.7 cm, $R_{10\%}$ =6.8 cm, V_{wind} = 5.5 m/sec			

Table A39. Test 69b (H = 8.5 cm, T = 2.0 sec, WL = 53.1 cm).

Gauge No.	H_{m0} (cm)	T_p (sec)	$\bar{\eta}$ (cm)
1	9.5	2.0	-0.3
2	8.5	2.0	-0.2
3	8.4	2.0	-0.2
4	6.6	2.1	-0.2
5	9.1	2.1	-0.3
6	8.6	2.1	-0.3
7	5.7	2.2	0.9
8	3.6	38.1	1.4
9	5.5	38.1	2.6
R_{max} = 8.0 cm, $R_{2\%}$ =7.1 cm, $R_{10\%}$ =6.1 cm, V_{wind} = 5.5 m/sec			

Table A40. Test 70b (H = 7.8 cm, T = 1.75 sec, WL = 53.1 cm).

Gauge No.	H_{m0} (cm)	T_p (sec)	$\bar{\eta}$ (cm)
1	8.6	1.8	-0.3
2	7.8	1.8	-0.2
3	7.7	1.8	-0.2
4	5.8	1.8	-0.2
5	8.1	1.8	-0.2
6	8.0	1.8	-0.3
7	5.3	1.8	0.8
8	3.0	38.1	1.3
9	4.7	38.1	2.4
R_{max} = 6.1 cm, $R_{2\%}$ =5.4 cm, $R_{10\%}$ =4.8 cm, V_{wind} = 5.3 m/sec			

Table A41. Test 71b (H = 7.5 cm, T = 1.5 sec, WL = 53.1 cm).

Gauge No.	H_{m0} (cm)	T_p (sec)	$\bar{\eta}$ (cm)
1	8.2	1.5	-0.2
2	7.5	1.5	-0.2
3	7.5	1.5	-0.2
4	5.4	1.5	-0.2
5	7.4	1.5	-0.2
6	7.8	1.5	-0.3
7	4.8	1.5	0.7
8	2.6	38.1	1.2
9	4.0	38.1	2.2
R_{max} = 4.9 cm, $R_{2\%}$ =3.9 cm, $R_{10\%}$ =3.7 cm, V_{wind} = 5.2 m/sec			

Table A42. Test 72b (H = 5.1 cm, T = 1.5 sec, WL = 53.1 cm).

Gauge No.	H_{m0} (cm)	T_p (sec)	$\bar{\eta}$ (cm)
1	5.5	1.5	-0.2
2	5.1	1.5	-0.1
3	5.1	1.5	-0.1
4	3.7	1.5	-0.1
5	5.2	1.5	-0.2
6	5.9	1.5	-0.2
7	4.0	1.5	0.4
8	2.0	38.1	0.8
9	3.4	38.1	1.6
R_{max} = 3.6 cm, $R_{2\%}$ =3.4 cm, $R_{10\%}$ =3.1 cm, V_{wind} = 4.4 m/sec			

Table A43. Test 73b (*H* = 6.0 cm, *T* = 1.25 sec, *WL* = 53.1 cm).

Gauge No.	H_{m0} (cm)	T_p (sec)	$\bar{\eta}$ (cm)
1	6.6	1.2	-0.2
2	6.0	1.2	-0.1
3	5.9	1.3	-0.2
4	4.2	1.2	-0.1
5	5.8	1.2	-0.2
6	6.3	1.2	-0.2
7	4.0	1.2	0.5
8	2.2	38.1	0.8
9	3.5	38.1	1.7
R$_{max}$ = 3.9 cm, R$_{2\%}$ =3.5 cm, R$_{10\%}$ =3.3 cm, *V*$_{wind}$ = 4.8 m/sec			

Table A44. Test 74b (*H* = 6.2 cm, *T* = 1.0 sec, *WL* = 53.1 cm).

Gauge No.	H_{m0} (cm)	T_p (sec)	$\bar{\eta}$ (cm)
1	6.8	1.0	-0.2
2	6.2	1.0	-0.1
3	6.2	1.0	-0.1
4	4.2	1.0	-0.1
5	5.6	1.0	-0.2
6	5.9	1.1	-0.1
7	3.8	1.1	0.4
8	2.1	8.8	0.8
9	3.1	38.1	1.6
R$_{max}$ = 4.6 cm, R$_{2\%}$ =3.4 cm, R$_{10\%}$ =3.1 cm, *V*$_{wind}$ = 4.5 m/sec			

Table A45. Test 75b (*H* = 3.4 cm, *T* = 1.0 sec, *WL* = 53.1 cm)

Gauge No.	H_{m0} (cm)	T_p (sec)	$\bar{\eta}$ (cm)
1	3.7	1.0	-0.1
2	3.4	1.0	0.0
3	3.4	1.0	0.0
4	2.5	1.0	0.0
5	3.4	1.0	-0.1
6	3.7	1.0	0.0
7	3.0	1.1	0.2
8	1.6	9.5	0.5
9	2.6	38.1	1.1
R$_{max}$ = 2.8 cm, R$_{2\%}$ =2.1 cm, R$_{10\%}$ =2.0 cm, *V*$_{wind}$ = 4.2 m/sec			

Table A46. Test 76b (H = 7.6 cm, T = 2.5 sec, WL = 50.0 cm).

Gauge No.	H_{m0} (cm)	T_p (sec)	$\bar{\eta}$ (cm)
1	8.4	2.5	-0.5
2	7.6	2.5	-0.4
3	7.6	2.5	-0.4
4	6.8	2.5	-0.4
5	8.5	2.4	-0.5
6	7.0	2.4	-0.3
7	3.5	2.5	1.5
8	2.3	57.1	2.0
9	4.6	38.1	3.9
R_{max} = 5.5 cm, $R_{2\%}$ =4.3 cm, $R_{10\%}$ =3.7 cm, V_{wind} = 1.9 m/sec			

Table A47. Test 77b (H = 8.3 cm, T = 2.0 sec, WL = 50.0 cm).

Gauge No.	H_{m0} (cm)	T_p (sec)	$\bar{\eta}$ (cm)
1	9.2	2.0	-0.5
2	8.3	2.0	-0.3
3	8.1	2.0	-0.3
4	6.9	2.0	-0.4
5	7.9	2.2	-0.4
6	6.7	2.2	-0.2
7	3.1	2.2	1.3
8	2.0	57.1	1.9
9	4.1	38.1	3.5
R_{max} = 5.1 cm, $R_{2\%}$ =3.9 cm, $R_{10\%}$ =3.2 cm, V_{wind} = 2.1 m/sec			

Table A48. Test 78b (H = 7.5 cm, T = 1.75 sec, WL = 50.0 cm).

Gauge No.	H_{m0} (cm)	T_p (sec)	$\bar{\eta}$ (cm)
1	8.2	1.8	-0.4
2	7.5	1.8	-0.3
3	7.3	1.8	-0.3
4	6.0	1.8	-0.3
5	7.1	1.8	-0.3
6	6.5	1.9	-0.2
7	2.8	1.8	1.1
8	1.6	57.1	1.7
9	3.2	38.1	3.2
R_{max} = 3.9 cm, $R_{2\%}$ =2.7 cm, $R_{10\%}$ =2.3 cm, V_{wind} = 2.1 m/sec			

Table A49. Test 79b (*H* = 6.7 cm, *T* = 1.5 sec, *WL* = 50.0 cm).

Gauge No.	H_{m0} (cm)	T_p (sec)	$\bar{\eta}$ (cm)
1	7.3	1.5	-0.3
2	6.7	1.5	-0.2
3	6.7	1.5	-0.2
4	5.2	1.5	-0.3
5	6.7	1.5	-0.4
6	6.3	1.5	-0.3
7	2.5	114.3	1.0
8	1.3	114.3	1.6
9	2.4	114.3	2.9
R_{max} = 1.3 cm, $R_{2\%}$ =1.1 cm, $R_{10\%}$ =1.0 cm, V_{wind} = 2.0 m/sec			

Table A50. Test 80b (*H* = 4.4 cm, *T* = 1.5 sec, *WL* = 50.0 cm).

Gauge No.	H_{m0} (cm)	T_p (sec)	$\bar{\eta}$ (cm)
1	4.8	1.5	-0.2
2	4.4	1.5	-0.2
3	4.4	1.5	-0.1
4	3.4	1.5	-0.2
5	4.6	1.4	-0.2
6	5.1	1.4	-0.3
7	1.8	114.3	0.7
8	1.0	114.3	1.2
9	1.7	114.3	2.1
R_{max} = 0.5 cm, $R_{2\%}$ =0.1 cm, $R_{10\%}$ =0.1 cm, V_{wind} = 1.8 m/sec			

Table A51. Test 81b (*H* = 5.1 cm, *T* = 1.25 sec, *WL* = 50.0 cm).

Gauge No.	H_{m0} (cm)	T_p (sec)	$\bar{\eta}$ (cm)
1	5.6	1.2	-0.2
2	5.1	1.2	-0.2
3	5.1	1.2	-0.1
4	3.8	1.2	-0.2
5	5.1	1.2	-0.3
6	5.1	1.2	-0.3
7	1.7	1.3	0.6
8	0.9	114.3	1.1
9	1.6	57.1	2.2
R_{max} = 0.3 cm, $R_{2\%}$ =0.0 cm, $R_{10\%}$ =0.0 cm, V_{wind} = 1.8 m/sec			

Table A52. Test 82b (*H* = 5.6 cm, *T* = 1.0 sec, *WL* = 50.0 cm).

Gauge No.	H_{m0} (cm)	T_p (sec)	$\bar{\eta}$ (cm)
1	6.1	1.0	-0.2
2	5.6	1.0	-0.1
3	5.6	1.0	-0.1
4	4.0	1.0	-0.2
5	5.1	1.0	-0.2
6	4.8	1.0	-0.2
7	1.5	28.6	0.6
8	0.8	114.3	1.0
9	1.3	57.1	2.0
R_{max} = 0.1 cm, $R_{2\%}$ =0.1 cm, $R_{10\%}$ =0.1 cm, V_{wind} = 1.4 m/sec			

Table A53. Test 83b (*H* = 2.9 cm, *T* = 1.0 sec, *WL* = 50.0 cm).

Gauge No.	H_{m0} (cm)	T_p (sec)	$\bar{\eta}$ (cm)
1	3.2	1.0	-0.2
2	2.9	1.0	-0.1
3	2.9	1.0	-0.1
4	2.1	1.0	-0.1
5	2.8	1.0	-0.2
6	3.1	1.0	-0.1
7	0.9	38.1	0.2
8	0.5	114.3	0.7
9	0.6	114.3	1.3
R_{max} = 0.0 cm, $R_{2\%}$ =0.0 cm, $R_{10\%}$ =0.0 cm, V_{wind} = 1.6 m/sec			

Table A54. Test 84 (*H* = 7.6 cm, *T* = 2.5 sec, *WL* = 50.0 cm).

Gauge No.	H_{m0} (cm)	T_p (sec)	$\bar{\eta}$ (cm)
1	8.4	2.5	-0.6
2	7.6	2.5	-0.4
3	7.6	2.5	-0.5
4	6.8	2.5	-0.4
5	8.7	2.4	-0.6
6	6.9	2.6	-0.3
7	3.1	2.5	1.4
8	2.3	57.1	2.3
9	4.6	38.1	4.5
R_{max} = 5.5 cm, $R_{2\%}$ =4.3 cm, $R_{10\%}$ =3.9 cm, V_{wind} = 5.4 m/sec			

Table A55. Test 85 (H = 8.2 cm, T = 2.0 sec, WL = 50.0 cm).

Gauge No.	H_{m0} (cm)	T_p (sec)	$\bar{\eta}$ (cm)
1	9.1	2.0	-0.5
2	8.2	2.0	-0.4
3	8.1	2.0	-0.4
4	6.9	2.0	-0.4
5	8.0	2.2	-0.4
6	6.7	2.2	-0.2
7	2.9	2.2	1.4
8	2.0	57.1	2.2
9	4.2	38.1	4.3
R_{max} = 5.2 cm, R$_{2\%}$ =4.0 cm, R$_{10\%}$ =3.3 cm, V_{wind} = 5.3 m/sec			

Table A56. Test 87 (H = 7.5 cm, T = 1.75 sec, WL = 50.0 cm).

Gauge No.	H_{m0} (cm)	T_p (sec)	$\bar{\eta}$ (cm)
1	8.2	1.8	-0.4
2	7.5	1.8	-0.3
3	7.3	1.8	-0.3
4	6.0	1.8	-0.3
5	7.2	1.8	-0.3
6	6.4	1.8	-0.3
7	2.7	1.8	1.2
8	1.7	57.1	2.0
9	3.3	38.1	3.9
R_{max} = 4.4 cm, R$_{2\%}$ =2.8 cm, R$_{10\%}$ =2.5 cm, V_{wind} = 3.8 m/sec			

Table A57. Test 88 (H = 6.8 cm, T = 1.5 sec, WL = 50.0 cm).

Gauge No.	H_{m0} (cm)	T_p (sec)	$\bar{\eta}$ (cm)
1	7.4	1.5	-0.4
2	6.8	1.5	-0.3
3	6.8	1.5	-0.3
4	5.3	1.5	-0.3
5	6.6	1.5	-0.3
6	6.2	1.4	-0.3
7	2.4	114.3	1.1
8	1.4	114.3	1.9
9	2.5	114.3	3.7
R_{max} = 1.9 cm, R$_{2\%}$ =1.6 cm, R$_{10\%}$ =1.6 cm, V_{wind} = 4.0 m/sec			

Table A58. Test 89 (*H* = 4.5 cm, *T* = 1.5 sec, *WL* = 50.0 cm).

Gauge No.	H_{m0} (cm)	T_p (sec)	$\bar{\eta}$ (cm)
1	4.9	1.5	-0.3
2	4.5	1.5	-0.2
3	4.5	1.5	-0.2
4	3.6	1.5	-0.2
5	4.7	1.4	-0.2
6	5.1	1.4	-0.3
7	1.8	114.3	0.7
8	1.0	114.3	1.5
9	1.8	114.3	2.9
R_{max} = 1.0 cm, $R_{2\%}$ =0.7 cm, $R_{10\%}$ =0.5 cm, V_{wind} = 3.7 m/sec			

Table A59. Test 90 (*H* = 5.3 cm, *T* = 1.25 sec, *WL* = 50.0 cm).

Gauge No.	H_{m0} (cm)	T_p (sec)	$\bar{\eta}$ (cm)
1	5.8	1.2	-0.3
2	5.3	1.2	-0.2
3	5.3	1.2	-0.2
4	4.0	1.2	-0.2
5	5.1	1.2	-0.2
6	5.1	1.2	-0.3
7	1.7	28.6	0.7
8	1.0	57.1	1.4
9	1.8	57.1	2.9
R_{max} = 1.0 cm, $R_{2\%}$ =0.7 cm, $R_{10\%}$ =0.5 cm, V_{wind} = 3.7 m/sec			

Table A60. Test 91 (*H* = 5.7 cm, *T* = 1.0 sec, *WL* = 50.0 cm).

Gauge No.	H_{m0} (cm)	T_p (sec)	$\bar{\eta}$ (cm)
1	6.3	1.0	-0.3
2	5.7	1.0	-0.2
3	5.8	1.0	-0.2
4	4.2	1.0	-0.2
5	5.2	1.0	-0.2
6	4.9	1.1	-0.2
7	1.5	8.2	0.6
8	0.9	14.3	1.4
9	1.5	57.1	2.8
R_{max} = 0.9 cm, $R_{2\%}$ =0.5 cm, $R_{10\%}$ =0.4 cm, V_{wind} = 5.3 m/sec			

Table A61. Test 92 (*H* = 3.1 cm, *T* = 1.0 sec, *WL* = 50.0 cm).

Gauge No.	H_{m0} (cm)	T_p (sec)	$\bar{\eta}$ (cm)
1	3.4	1.0	-0.3
2	3.1	1.0	-0.1
3	3.2	1.0	-0.3
4	2.4	1.0	-0.1
5	3.1	1.0	-0.1
6	3.5	1.0	-0.2
7	1.0	14.3	0.3
8	0.6	114.3	0.9
9	0.9	114.3	1.9
R_{max} = 0.3 cm, R$_{2\%}$ =0.3 cm, R$_{10\%}$ =0.3 cm, V_{wind} = 5.3 m/sec			

Table A62. Test 94 (*H* = 7.6 cm, *T* = 2.5 sec, *WL* = 50.0 cm).

Gauge No.	H_{m0} (cm)	T_p (sec)	$\bar{\eta}$ (cm)
1	8.5	2.5	-0.6
2	7.6	2.5	-0.4
3	7.7	2.5	-0.5
4	7.0	2.5	-0.4
5	8.9	2.4	-0.5
6	6.9	2.6	-0.2
7	3.5	2.5	1.6
8	2.4	57.1	2.5
9	4.6	38.1	5.1
R_{max} = 5.9 cm, R$_{2\%}$ =5.3 cm, R$_{10\%}$ =4.5 cm, V_{wind} = 5.4 m/sec			

Table A63. Test 95 (*H* = 8.3 cm, *T* = 2.0 sec, *WL* = 50.0 cm).

Gauge No.	H_{m0} (cm)	T_p (sec)	$\bar{\eta}$ (cm)
1	9.3	2.0	-0.6
2	8.3	2.0	-0.4
3	8.2	2.0	-0.4
4	7.0	2.0	-0.4
5	8.4	2.0	-0.4
6	6.7	2.2	-0.1
7	3.1	2.2	1.5
8	2.1	57.1	2.4
9	4.1	38.1	4.9
R_{max} = 5.5 cm, R$_{2\%}$ =3.9 cm, R$_{10\%}$ =3.4 cm, V_{wind} = 5.6 m/sec			

Table A64. Test 96 (*H* = 7.6 cm, *T* = 1.75 sec, *WL* = 50.0 cm).

Gauge No.	H_{m0} (cm)	T_p (sec)	$\bar{\eta}$ (cm)
1	8.5	1.8	-0.5
2	7.6	1.8	-0.4
3	7.5	1.8	-0.4
4	6.3	1.8	-0.3
5	7.6	1.8	-0.4
6	6.4	1.9	-0.2
7	2.8	114.3	1.3
8	1.7	57.1	2.2
9	3.5	38.1	4.6
R_{max} = 4.8 cm, $R_{2\%}$ =3.1 cm, $R_{10\%}$ =2.7 cm, V_{wind} = 5.2 m/sec			

Table A65. Test 97 (*H* = 7.0 cm, *T* = 1.5 sec, *WL* = 50.0 cm).

Gauge No.	H_{m0} (cm)	T_p (sec)	$\bar{\eta}$ (cm)
1	7.6	1.5	-0.5
2	7.0	1.5	-0.3
3	7.0	1.5	-0.4
4	5.5	1.5	-0.3
5	7.0	1.5	-0.4
6	6.0	1.4	-0.3
7	2.4	114.3	1.2
8	1.4	114.3	2.1
9	2.6	57.1	4.4
R_{max} = 2.6 cm, $R_{2\%}$ =2.0 cm, $R_{10\%}$ =1.8 cm, V_{wind} = 7.1 m/sec			

Table A66. Test 98 (*H* = 4.7 cm, *T* = 1.5 sec, *WL* = 50.0 cm).

Gauge No.	H_{m0} (cm)	T_p (sec)	$\bar{\eta}$ (cm)
1	5.2	1.5	-0.4
2	4.7	1.5	-0.3
3	4.7	1.5	-0.3
4	4.0	1.5	-0.2
5	5.2	1.5	-0.3
6	5.2	1.4	-0.3
7	1.8	114.3	0.8
8	1.1	114.3	1.8
9	2.0	57.1	3.7
R_{max} = 1.5 cm, $R_{2\%}$ =1.0 cm, $R_{10\%}$ =0.9 cm, V_{wind} = 7.1 m/sec			

Table A67. Test 99 (H = 5.5 cm, T = 1.25 sec, WL = 50.0 cm).

Gauge No.	H_{m0} (cm)	T_p (sec)	$\bar{\eta}$ (cm)
1	6.0	1.2	-0.4
2	5.5	1.2	-0.3
3	5.5	1.2	-0.3
4	4.4	1.2	-0.2
5	5.7	1.2	-0.3
6	5.1	1.2	-0.2
7	1.8	1.2	0.8
8	1.0	57.1	1.7
9	2.0	57.1	3.6
R_{max} = 1.5 cm, $R_{2\%}$ =1.1 cm, $R_{10\%}$ =1.0 cm, V_{wind} = 7.1 m/sec			

Table A68. Test 100 (H = 6.0 cm, T = 1.0 sec, WL = 50.0 cm).

Gauge No.	H_{m0} (cm)	T_p (sec)	$\bar{\eta}$ (cm)
1	6.5	1.0	-0.4
2	6.0	1.0	-0.3
3	6.1	1.0	-0.4
4	4.6	1.0	-0.2
5	5.8	1.0	-0.3
6	4.9	1.0	-0.2
7	1.6	22.9	0.7
8	1.0	14.3	1.7
9	1.8	57.1	3.7
R_{max} = 1.6 cm, $R_{2\%}$ =1.2 cm, $R_{10\%}$ =1.1 cm, V_{wind} = 6.9 m/sec			

Table A69. Test 101 (H = 3.3 cm, T = 1.0 sec, WL = 50.0 cm).

Gauge No.	H_{m0} (cm)	T_p (sec)	$\bar{\eta}$ (cm)
1	3.6	1.0	-0.3
2	3.3	1.0	-0.2
3	3.4	1.0	-0.3
4	2.9	1.0	-0.1
5	3.8	1.0	-0.2
6	3.8	1.0	-0.2
7	1.0	114.3	0.4
8	0.7	114.3	1.4
9	1.4	114.3	3.3
R_{max} = 0.7 cm, $R_{2\%}$ =0.5 cm, $R_{10\%}$ =0.5 cm, V_{wind} = 5.3. m/sec			

Table A70. Test 102 (H = 8.2 cm, T = 2.5 sec, WL = 53.1 cm).

Gauge No.	H_{m0} (cm)	T_p (sec)	$\bar{\eta}$ (cm)
1	9.2	2.5	-0.4
2	8.2	2.5	-0.3
3	8.3	2.5	-0.3
4	6.8	2.5	-0.3
5	9.9	2.5	-0.5
6	9.1	2.6	-0.4
7	6.2	2.6	1.0
8	4.0	38.1	1.7
9	5.6	38.1	3.1
R_{max} = 8.4 cm, $R_{2\%}$ =8.4 cm, $R_{10\%}$ =7.9 cm, V_{wind} = 7.0 m/sec			

Table A71. Test 103 (H = 8.6 cm, T = 2.0 sec, WL = 53.1 cm).

Gauge No.	H_{m0} (cm)	T_p (sec)	$\bar{\eta}$ (cm)
1	9.6	2.0	-0.4
2	8.6	2.0	-0.2
3	8.5	2.0	-0.3
4	6.8	2.1	-0.2
5	9.2	2.1	-0.3
6	8.6	2.1	-0.3
7	5.7	2.2	1.0
8	3.6	38.1	1.7
9	5.1	38.1	3.0
R_{max} = 7.8 cm, $R_{2\%}$ =7.5 cm, $R_{10\%}$ =6.4 cm, V_{wind} = 7.1 m/sec			

Table A72. Test 104 (H = 8.0 cm, T = 1.75 sec, WL = 53.1 cm).

Gauge No.	H_{m0} (cm)	T_p (sec)	$\bar{\eta}$ (cm)
1	8.9	1.8	-0.4
2	8.0	1.8	-0.2
3	8.0	1.8	-0.4
4	6.1	1.8	-0.2
5	8.6	1.8	-0.2
6	8.1	1.8	-0.2
7	5.2	1.8	0.8
8	3.0	38.1	1.5
9	4.3	38.1	2.8
R_{max} = 6.7 cm, $R_{2\%}$ =5.9 cm, $R_{10\%}$ =5.3 cm, V_{wind} = 5.8 m/sec			

Table A73. Test 105 (*H* = 7.8 cm, *T* = 1.5 sec, *WL* = 53.1 cm).

Gauge No.	H_{m0} (cm)	T_p (sec)	$\bar{\eta}$ (cm)
1	8.6	1.5	-0.3
2	7.8	1.5	-0.2
3	7.9	1.5	-0.2
4	5.7	1.5	-0.2
5	8.0	1.5	-0.2
6	8.0	1.5	-0.3
7	4.8	1.4	0.8
8	2.6	38.1	1.4
9	3.8	38.1	2.7
R_{max} = 5.9 cm, R$_{2\%}$ =4.5 cm, R$_{10\%}$ =4.1 cm, V_{wind} = 6.3 m/sec			

Table A74. Test 106 (*H* = 5.4 cm, T = 1.5 sec, *WL* = 53.1 cm).

Gauge No.	H_{m0} (cm)	T_p (sec)	$\bar{\eta}$ (cm)
1	5.8	1.5	-0.2
2	5.4	1.5	-0.1
3	5.3	1.5	-0.1
4	4.1	1.5	-0.1
5	5.7	1.5	-0.1
6	6.2	1.5	-0.1
7	4.1	1.5	0.5
8	2.1	38.1	1.0
9	3.3	38.1	2.0
R_{max} = 4.0 cm, R$_{2\%}$ =3.5 cm, R$_{10\%}$ =3.2 cm, V_{wind} = 6.7 m/sec			

Table A75. Test 107 (*H* = 6.3 cm, *T* = 1.25 sec, *WL* = 53.1 cm).

Gauge No.	H_{m0} (cm)	T_p (sec)	$\bar{\eta}$ (cm)
1	6.9	1.2	-0.3
2	6.3	1.2	-0.1
3	6.2	1.2	-0.2
4	4.5	1.2	-0.1
5	6.3	1.2	-0.2
6	6.6	1.2	-0.2
7	4.2	1.2	0.6
8	2.3	38.1	1.1
9	3.4	38.1	2.2
R_{max} = 4.5 cm, R$_{2\%}$ =3.9 cm, R$_{10\%}$ =3.6 cm, V_{wind} = 6.8 m/sec			

Table A76. Test 108 (*H* = 6.6 cm, *T* = 1.0 sec, *WL* = 53.1 cm).

Gauge No.	H_{m0} (cm)	T_p (sec)	$\bar{\eta}$ (cm)
1	7.2	1.0	-0.2
2	6.6	1.0	-0.1
3	6.6	1.0	-0.1
4	4.6	1.0	-0.1
5	6.3	1.0	-0.2
6	6.3	1.1	-0.1
7	3.9	1.1	0.6
8	2.3	8.8	1.1
9	3.2	38.1	2.1
R_{max} = 6.4 cm, $R_{2\%}$ =3.8 cm, $R_{10\%}$ =3.7 cm, V_{wind} = 6.7 m/sec			

Table A77. Test 109 (*H* = 3.8 cm, *T* = 1.0 sec, *WL* = 53.1 cm).

Gauge No.	H_{m0} (cm)	T_p (sec)	$\bar{\eta}$ (cm)
1	4.1	1.0	-0.2
2	3.8	1.0	-0.1
3	3.8	1.0	-0.1
4	2.9	1.0	0.0
5	4.0	1.0	0.0
6	4.3	1.0	0.0
7	3.2	1.1	0.3
8	1.8	9.5	0.8
9	2.8	38.1	1.6
R_{max} = 5.3 cm, $R_{2\%}$ =3.1 cm, $R_{10\%}$ =2.9 cm, V_{wind} = 6.5 m/sec			

Table A78. Test Wind-cal-U1 (*WL* = 53.1 cm).

Gauge No.	H_{m0} (cm)	T_p (sec)	$\bar{\eta}$ (cm)
1	0.2	0.2	-0.1
2	0.2	0.2	0.0
3	0.2	0.2	0.0
4	0.2	0.2	0.0
5	0.2	0.2	-0.1
6	0.3	0.2	0.0
7	-	-	-
8	0.4	0.7	0.0
9	0.3	0.3	0.0
R_{max} = 0.0 cm, $R_{2\%}$ =0.0 cm, $R_{10\%}$ =0.0 cm, V_{wind} = 0.95 m/sec			

Table A79. Test Wind-cal-U2 (*WL* = 53.1 cm).

Gauge No.	H_{m0} (cm)	T_p (sec)	$\bar{\eta}$ (cm)
1	0.2	0.3	-0.1
2	0.2	0.6	0.0
3	0.3	0.7	0.0
4	0.2	0.2	0.0
5	-	-	-
6	0.4	0.2	0.0
7	0.6	0.3	0.0
8	0.4	0.2	0.1
9	0.3	0.2	0.1
R_{max} = 0.0 cm, R_{2%} =0.0 cm, R_{10%} =0.0 cm, V_{wind} = 2.0 m/sec			

Table A80. Test Wind-cal-U3 (*WL* = 53.1 cm).

Gauge No.	H_{m0} (cm)	T_p (sec)	$\bar{\eta}$ (cm)
1	0.4	0.2	-0.2
2	0.4	0.2	0.0
3	0.5	0.2	0.0
4	0.5	0.2	0.1
5	0.9	0.2	0.1
6	0.9	0.2	0.0
7	-	-	-
8	0.9	0.3	0.1
9	1.1	0.3	0.2
R_{max} = 0.2 cm, R_{2%} =0.2 cm, R_{10%} =0.2 cm, V_{wind} = 3.1 m/sec			

Table A81. Test Wind-cal-U4 (*WL* = 53.1 cm).

Gauge No.	H_{m0} (cm)	T_p (sec)	$\bar{\eta}$ (cm)
1	0.7	0.2	-0.3
2	0.7	0.2	0.0
3	0.7	0.2	-0.1
4	0.8	0.3	0.1
5	1.3	0.3	-0.1
6	1.4	0.3	0.0
7	1.4	0.3	0.1
8	1.1	0.3	0.2
9	1.3	0.3	0.3
R_{max} = 0.3 cm, R_{2%} =0.3 cm, R_{10%} =0.3 cm, V_{wind} = 4.0 m/sec			

Table A82. Test Wind-cal-U5 (*WL* = 53.1 cm).

Gauge No.	H_{m0} (cm)	T_p (sec)	$\bar{\eta}$ (cm)
1	1.0	0.2	-0.1
2	1.0	0.2	0.0
3	1.0	0.2	-0.1
4	1.1	0.3	0.0
5	1.8	0.3	-0.1
6	1.7	0.3	0.0
7	1.6	0.4	0.1
8	1.1	0.4	0.2
9	2.2	0.4	0.5
R_{max} = 0.5 cm, R$_{2\%}$ =0.4 cm, R$_{10\%}$ =0.4 cm, V_{wind} = 4.7 m/sec			

Table A83. Test Wind-cal-U6 (*WL* = 53.1 cm).

Gauge No.	H_{m0} (cm)	T_p (sec)	$\bar{\eta}$ (cm)
1	1.1	0.2	-0.6
2	1.3	0.3	0.0
3	1.3	0.2	-0.2
4	1.4	0.3	0.0
5	2.1	0.3	-0.1
6	2.2	0.4	0.0
7	1.8	0.4	0.1
8	1.3	0.4	0.3
9	2.4	0.5	0.7
R_{max} = 0.6 cm, R$_{2\%}$ =0.6 cm, R$_{10\%}$ =0.6 cm, V_{wind} = 5.4 m/sec			

Table A84. Test Wind-cal-U7 (*WL* = 53.1 cm).

Gauge No.	H_{m0} (cm)	T_p (sec)	$\bar{\eta}$ (cm)
1	1.8	0.3	-0.6
2	1.7	0.3	0.0
3	1.6	0.3	-0.4
4	1.7	0.4	0.0
5	2.5	0.4	0.0
6	2.8	0.4	0.0
7	2.0	0.4	0.1
8	1.5	0.4	0.4
9	2.6	0.5	0.9
R_{max} = 1.2 cm, R$_{2\%}$ =1.2 cm, R$_{10\%}$ =1.1 cm, V_{wind} =6.3m/sec			

Table A85. Test Wind-cal4-U3 (*WL* = 53.1 cm).

Gauge No.	H_{m0} (cm)	T_p (sec)	$\bar{\eta}$ (cm)
1	0.4	0.2	0.0
2	0.4	0.2	0.1
3	0.5	0.2	0.1
4	0.5	0.2	0.0
5	0.8	0.2	0.0
6	0.8	0.2	0.0
7	0.9	0.2	0.2
8	0.7	0.3	0.2
9	0.5	2.9	0.2
R_{max} = 0.1 cm, $R_{2\%}$ =0.1 cm, $R_{10\%}$ =0.1 cm, V_{wind} = 2.7 m/sec			

Table A86. Test Wind-cal4-U6 (*WL* = 53.1 cm).

Gauge No.	H_{m0} (cm)	T_p (sec)	$\bar{\eta}$ (cm)
1	1.3	0.2	-0.1
2	1.4	0.2	0.0
3	1.3	0.2	0.0
4	1.3	0.3	0.0
5	2.1	0.4	0.0
6	2.3	0.4	0.0
7	1.9	0.4	0.2
8	1.5	0.4	0.4
9	2.7	0.4	0.8
R_{max} = 0.7 cm, $R_{2\%}$ =0.7 cm, $R_{10\%}$ =0.7 cm, V_{wind} = 4.6 m/sec			

Table A87. Test Wind-cal4-U8 (*WL* = 53.1 cm).

Gauge No.	H_{m0} (cm)	T_p (sec)	$\bar{\eta}$ (cm)
1	2.1	0.3	-0.2
2	2.1	0.3	0.0
3	2.1	0.3	-0.1
4	2.0	0.4	0.0
5	3.0	0.4	0.1
6	3.2	0.4	0.0
7	2.2	0.4	0.3
8	1.6	0.5	0.6
9	3.0	0.5	1.4
R_{max} = 1.8 cm, $R_{2\%}$ =1.4 cm, $R_{10\%}$ =1.4 cm, V_{wind} = 5.9 m/sec			

REPORT DOCUMENTATION PAGE			Form Approved OMB No. 0704-0188

Public reporting burden for this collection of information is estimated to average 1 hour per response, including the time for reviewing instructions, searching existing data sources, gathering and maintaining the data needed, and completing and reviewing this collection of information. Send comments regarding this burden estimate or any other aspect of this collection of information, including suggestions for reducing this burden to Department of Defense, Washington Headquarters Services, Directorate for Information Operations and Reports (0704-0188), 1215 Jefferson Davis Highway, Suite 1204, Arlington, VA 22202-4302. Respondents should be aware that notwithstanding any other provision of law, no person shall be subject to any penalty for failing to comply with a collection of information if it does not display a currently valid OMB control number. **PLEASE DO NOT RETURN YOUR FORM TO THE ABOVE ADDRESS.**

1. REPORT DATE (DD-MM-YYYY) July 2007	2. REPORT TYPE Report 1 of a Series	3. DATES COVERED (From - To)

4. TITLE AND SUBTITLE Laboratory Study of Wind Effect on Runup over Fringing Reefs; Report 1: Data Report	5a. CONTRACT NUMBER
	5b. GRANT NUMBER
	5c. PROGRAM ELEMENT NUMBER
6. AUTHOR(S) Zeki Demirbilek, Okey G. Nwogu, and Donald L. Ward	5d. PROJECT NUMBER
	5e. TASK NUMBER
	5f. WORK UNIT NUMBER

7. PERFORMING ORGANIZATION NAME(S) AND ADDRESS(ES) Coastal and Hydraulics Laboratory, U.S. Army Engineer Research and Development Center, 3909 Halls Ferry Road, Vicksburg, MS 39180-6199; University of Michigan, Department of Naval Architecture and Marine Engineering, 2600 Draper Road, Ann Arbor, MI 48109-2145	8. PERFORMING ORGANIZATION REPORT NUMBER ERDC/CHL TR-07-4

9. SPONSORING / MONITORING AGENCY NAME(S) AND ADDRESS(ES) U.S. Army Corps of Engineers Washington, DC 20314-1000	10. SPONSOR/MONITOR'S ACRONYM(S)
	11. SPONSOR/MONITOR'S REPORT NUMBER(S)

12. DISTRIBUTION / AVAILABILITY STATEMENT
Approved for public release; distribution is unlimited.

13. SUPPLEMENTARY NOTES
Accompanying raw data files are posted at the Coastal Inlets Research Program (CIRP) Web site (*http://cirp.wes.army.mil/cirp/cirp.html*)

14. ABSTRACT

The report describes experimental data obtained from a wind-wave flume study conducted August-September 2006 at the University of Michigan in Ann Arbor, MI. The study objectives were two-fold: to quantify wind effects on wave runup on fringing reefs of the Pacific Island of Guam and to obtain detailed wave data along a complex reef system consisting of steep slopes and shallow areas for validating wave breaking, dissipation, wave setup and runup capabilities of a Boussinesq-type wave model. An idealized 1:64 model of a two-dimensional fringing reef, representative of the reef systems along the southeast coast of island of Guam, was built in the flume. The reef cross-sectional profile consisted of a beach, a flat and wide reef section, and a reef face with composite slope.

The reef profile was built from a relatively smooth and impervious plastic material (polyvinyl chloride). The wind generator and wave-maker mechanisms were located at opposite ends of the test flume. Eleven probes (gauges) collected time series surface elevation and wind speed data. Tests were performed without wind (waves-only), with wind-only, and with both waves and wind together. Data obtained in this study will be used in the calibration of numerical models to estimate wave setup and runup affecting the flooding of Pacific islands.

(Continued)

15. SUBJECT TERMS		
Fringing reefs Reflection and spectral analyses	Surge and wave modeling Time-series data	Wave runup and setup Wind effects

16. SECURITY CLASSIFICATION OF:			17. LIMITATION OF ABSTRACT	18. NUMBER OF PAGES	19a. NAME OF RESPONSIBLE PERSON
a. REPORT UNCLASSIFIED	b. ABSTRACT UNCLASSIFIED	c. THIS PAGE UNCLASSIFIED		82	19b. TELEPHONE NUMBER (include area code)

Standard Form 298 (Rev. 8-98)
Prescribed by ANSI Std. 239.18

14. ABSTRACT (continued)

This data report describes the experiment and data. Subsequent reports are expected to address the analyses and use of data and numerical modeling studies. General features of the experiment are summarized in the report, including description of test facility, instrumentation, test conditions, and preliminary results. Raw data are provided on the Coastal Inlets Research Program (CIRP) Web site (*http://cirp.wes.army.mil/cirp/cirp.html*). The analyzed data are presented in Appendix A of this report for each test at nine wave probes, runup gauge and hot-wire anemometer. Values of measured significant wave height, peak wave period, mean water level, and wind speed are provided. The maximum runup, R_{max}, is calculated as maximum vertical excursion of the water level at the shoreline (runup gauge) relative to the still-water level. The runup levels exceeded by 2 percent ($R_{2\%}$) and 10 percent ($R_{10\%}$) of the runup peaks are also tabulated.